Understanding Important Drivers for Carbonyl Sulfide (OCS) Soil Fluxes

Master Thesis

author
Enpei Li

supervisor
Prof. dr. Maarten Krol

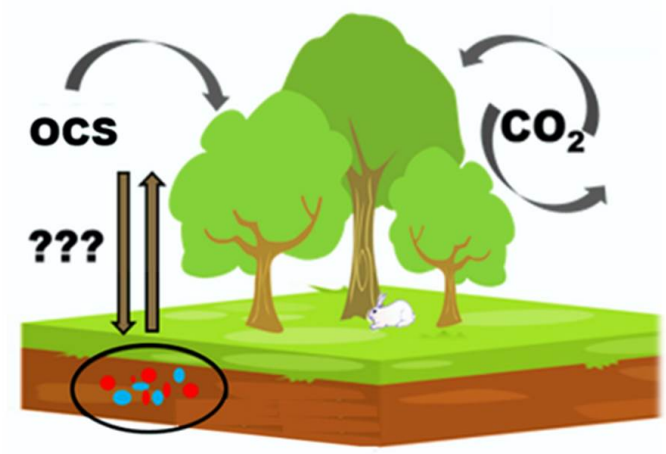

June, 2018

Wageningen University and Research

Document title: Understanding Important Drivers for Carbonyl Sulfide (OCS) Soil Fluxes

Master thesis for the MSc programme Environmental Sciences at Wageningen University in the thesis track of Air Quality & Atmospheric Chemistry

Date: July, 2018

Author: Enpei Li
enpei.li@outlook.com

Assessment committee: Prof. dr. Maarten Krol
Prof. dr. Wouter Peters

Wageningen University: Meteorology and Air Quality Group

Abstract

Carbonyl sulfide (OCS or COS) is proposed as a proxy for photosynthesis, for its similarity with CO_2 in the structure and the vegetation sink. While CO_2 is involved in autotrophic respiration there is no observed respiration-like OCS emission from vegetation. When using OCS to partition the photosynthetic CO_2 flux beyond the leaf scale, the quantification of soil-atmosphere OCS exchange is important. While both uptake and emission are known to coexist in the soil, soils mainly act as an OCS sink. The balance between uptake and emission is dependent on environmental conditions.

In this thesis, we built a soil-atmosphere OCS exchange model to better understand the OCS soil fluxes based on two recent OCS flux models: one is depth-resolved and the other is steady-state solution. We were able to reproduce the main features of the change of soil OCS fluxes with the drivers, such as the source-sink transition and the diurnal variations of soil-atmosphere exchange with temperature. We found that temperature is the most important driver for soil OCS fluxes by affecting both the uptake and emission processes. Moreover, the uptake of OCS is linearly correlated with atmospheric OCS concentration. The OCS soil processes are largely diffusion limited in non-steady-state situations, while the steady-state fluxes are mostly influenced by the enzyme activity in the uppermost soil layers.

Contents

1 Introduction **1**

2 Processes and drivers involved in OCS soil fluxes **3**
2.1 Diffusion and dissolution of OCS in the soil 3
2.2 Mechanisms of uptake and production of OCS 4
2.2.1 OCS uptake mechanisms 4
2.2.2 OCS production mechanisms 5

3 Model description **6**
3.1 Parameterization of the processes 6
3.1.1 Diurnal variation of temperature 6
3.1.2 Parameterization of diffusion and dissolution of OCS in the soil . . 7
3.1.3 Parameterization of soil OCS uptake and production 7
3.2 Model description of the column model 8
3.2.1 Temperature and moisture dependency in the Sun model 8
3.2.2 Vertical discretization of the column model 8
3.2.3 Set-ups of the base run 10
3.3 Model description of the steady-state model 10
3.3.1 Steady-state solution of the Ogée model 10

4 Results: modeled OCS processes in the column model **12**
4.1 Time steps for eliminating fluctuations 12
4.2 Drivers of OCS diffusion in the soil 13
4.2.1 Soil porosity 14
4.2.2 Soil temperature 14
4.2.3 Soil moisture 15
4.3 Drivers of OCS source in the soil 16
4.3.1 Coupling of the source term 16
4.3.2 OCS Source strength and soil temperature 17
4.4 Drivers of OCS sink in the soil 18
4.4.1 Coupling of the sink term 18
4.4.2 Ambient OCS concentration and the hydrolysis rate 18
4.4.3 Soil temperature & moisture and the hydrolysis rate 19

5 Soil OCS flux sensitivity to different drivers in the column model **21**
5.1 Soil temperature and the sink to source transition 21
5.2 Compensation concentration and the sink to source transition 24

6 Reproduce the steady-state solution with the column model **26**
6.1 Set-up of the new Sun model 26
6.2 Comparison of the outputs from the new Sun model and from the Ogée model 26
6.2.1 Comparison of the responses of the OCS fluxes to the dynamical temperature 27
6.2.2 OCS soil fluxes' responses to the temperature change after steady-state 28
6.3 Vertical profile of source and sink 28

6.3.1 Effects of an extra deep OCS source in the soil 29

7 Discussion **30**

8 Conclusions **31**

9 Recommendations **31**

References **34**

Appendix A Appendix **38**

Appendix A.1 Temperature dependency of uptake term in the Sun & the Ogée model 38

Appendix A.2 Soil moisture and the sink to source transition 40

Appendix A.3 Compensation concentration in the Ogée model 41

Appendix B Code of the models **41**

1. Introduction

Warming of the climate system is undeniable: last three decades have been successively warmer at the Earth's surface than other decades since 1850. Climate change puts people, societies, economic sectors and ecosystems at risk, from brief events such as severe storms to slow trends such as droughts or sea level rise.[1] Climate models are useful tools for analyzing and predicting climate related risk. However, there is a disagreement among climate models on how much CO_2 the land ecosystems can take up for photosynthesis, owing to the inability to study the simultaneous photosynthesis and autotrophic respiration separately beyond the leaf scale[2]. The terrestrial biosphere, which absorbs a quarter of the CO_2 released by anthropogenic activities to the atmosphere, is an integral component of the carbon cycle and the climate system[3]. Functioning of the terrestrial biosphere can be strongly affected by climate change: e.g.the assumed increasing climate extreme events may reduce photosynthesis or increase respiration[4].

For these reasons, it is important to separate these carbon fluxes to quantify the carbon storage and predict the sensitivity of the system[5]. Here, carbonyl sulfide (OCS or COS) can provide new clues. OCS is the most abundant volatile reduced sulfur compound and nearly inert to photochemical decomposition in the troposphere, with a rather uniform mixing ratio of approximately 500 ppt (10^{-12}), and a lifetime ~2.5 yr[6, 7]. OCS was studied extensively in the 1990s for its stratospheric process, as OCS transported to and oxidized in the stratosphere is believed to be the major source of stratospheric background sulfur aerosol[8]. These aerosols influence the radiation budget and the stratospheric ozone cycle, hence the climate[9].

Recently, there is an increasing interest to use OCS as a proxy to constrain ecosystem gross primary productivity (GPP) for its similarity to CO_2[10, 2, 11]. OCS and CO_2 diffuse into leaves along a similar pathway through the stomata to the mesophyll, where they react with enzymes, mainly carbonic anhydrase (CA)[12, 13]. With no respiration-like OCS emissions from actively photosynthesizing vegetation[10], uptake of OCS can therefore be used as a direct proxy of the photosynthetic CO_2 uptake. The key enzyme for OCS uptake (CA) is a ubiquitous zinc enzyme which also accelerates the reversible hydration of CO_2[14]. CA also occurs in soil organisms, thus OCS that diffuses into the soil can be hydrolyzed[15, 16].

Soil-atmosphere OCS exchange is normally negligible compared to plant uptake. However, taking OCS soil fluxes into account is still important to avoid over- and underestimations when estimating GPP beyond the leaf scale[11]. In some cases, the soil flux can even be dominant in the ecosystem OCS flux[17]. The estimations of overall flux of OCS from atmosphere to soils markedly differ[8, 6]. While soils are observed to act as OCS sink globally, soils sources were observed over agriculture fields and anoxic soils[18], but there are also reported OCS sources over well-aerated soils[17]. Therefore there are unknowns in the soil processes of OCS. Whether the soil acts as a source or a sink for OCS depends on the physical, chemical and biological conditions of the soil, which control the coexisting uptake or emission of OCS. These conditions are called "drivers", such as soil temperature, moisture, etc.

Recently, two modeling frameworks were developed to describe the soil OCS flux, with similar drivers as input[18, 19]. The Sun model[19] resolves the soil column explicitly for

reproducing field observations, while the Ogée model[18] derives an analytical steady-state solution, suitable for reproducing lab experiments. The parameterization of these processes in the models remain largely empirical, and some important drivers (e.g. light-driven OCS production) are lacking[18]. Still, these models are important for identifying which drivers need to be focused on.

Important drivers need to be identified to integrate the OCS flux model to more comprehensive land-surface models[19], or to upscale the OCS exchange model. This can provide information for future studies for estimation of global soil OCS budget by integrating the soil OCS exchange into global land models (e.g. Community Land Model or Simple Biosphere Model).

The objectives of this thesis are two-fold: 1) to reproduce the mechanistic frameworks of Sun et al.[19] and Ogée et al.[18] for OCS exchange between atmosphere and soil; 2) to use the models as a tool to identify the important drivers for OCS soil-atmosphere exchange. The following research questions are guiding the thesis:

1. How does soil-atmosphere OCS exchange depend on vertical soil profiles of production and uptake?
2. What is the model's ability to reproduce observed exchange fluxes and vertical profiles under various environmental conditions?
3. What are the important drivers that determine OCS exchange (T, enzyme activity, and soil water content)?
4. Given the need to upscale the soil-atmosphere exchange to global scales, what are the important factors to consider?

The last question will be addressed by contrasting the depth-resolved Sun model[19] and a deposition-velocity based approach by Ogée et al[18].OCS soil processes need to be considered first to answer the questions about the drivers. In the following chapter, more theoretical details are introduced.

2. Processes and drivers involved in OCS soil fluxes

The uptake or emission of gases in soil systems is mainly controlled by the physical, chemical and biological processes in the vadose zone[20]. For OCS, we consider diffusion (physical), dissolution (chemical) and loss-production (chemical and biological) in the soil column as main processes. Figure 1 described important drivers of OCS soil processes. These processes are strongly linked to soil properties, thus we define those physical and chemical properties as drivers for OCS fluxes. The drivers discussed here are soil temperature (T), soil water content (SWC or moisture), soil porosity (θ), CA activity (which is affected by both T and SWC).

Gas diffusion plays an important role in the soil-atmosphere OCS exchange as diffusivity acts as a limiting factor for OCS uptake[21]. OCS needs to reach microbial cells by diffusion before it can be consumed or produced through biotic processes (Figure 1). Diffusion is influenced by water-filled pore space as the pores can be blocked by the water. However, as OCS can dissolve in water, the water does not strictly block the transport. Both biotic and abiotic consumption and production processes exist in soil, which are affected by different drivers.

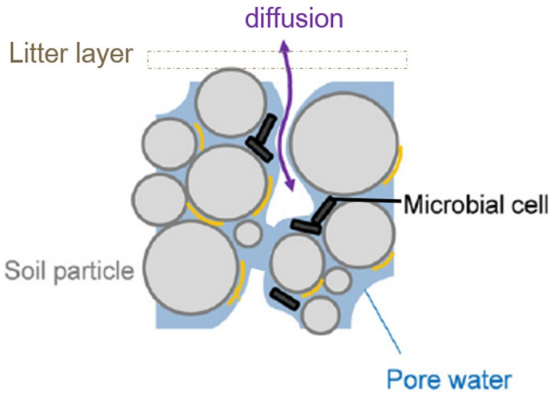

Figure 1: Schematic illustration of drivers' effects on OCS soil fluxes, after Moyano et al.[22].

2.1. Diffusion and dissolution of OCS in the soil

Diffusion processes in the soil water and air phases often govern the transport[23]. This is also the case for OCS as it can dissolve in the water. The transport of OCS affects the availability of OCS for uptake and exchange. Thus we firstly discuss the diffusion and dissolution, then the uptake and production.

Soil porosity, moisture and temperature are the important drivers for diffusion. In general, larger pores allow more rapid movements of gas than smaller pores[24]. Compaction and water saturation of soils are the main barriers to soil gas transport, with water being a more effective barrier. The diffusion of gases in water is slower than that in air by a factor of 10 000[25]. Moreover, a higher temperature allows the molecules to move faster.

For dissolution of OCS, the solubility is 80 (volume per 100 volumes of water) at 1 atm and 13.5 °C, less soluble than CO_2. OCS reacts slowly with water and produces CO_2 and H_2S[26]. The dissolution of gas is commonly described by Henry's law[27]: the amount

of dissolved gas is proportional to its partial pressure in the gas phase. Fick's law relates the unsteady (non-stationary) diffusive flux to the concentration gradient[28]. Combining Henry's law with Fick's law, we can describe the diffusion and dissolution of OCS in the mass balance equation[19]:

$$\frac{\partial C}{\partial t}[(k_H\theta_w + \theta_a)] = \frac{\partial}{\partial z}(D\frac{\partial C}{\partial z}) + P - U \quad (1)$$

where C (mol m^{-3}) is the gas concentration OCS; k_H is the dimensionless Henry's law constant (dissolution fraction), D (m^2 s^{-1}) is the effective OCS diffusivity in soil, P and U are respectively production and loss term (mol m^{-3} s^{-1}) (which is further explained in section 2.2), θ_w is the water-filled porosity and θ_a the air-filled porosity (both in m^3 m^{-3} soil).

2.2. Mechanisms of uptake and production of OCS

Uptake and production of OCS coexist in the soil as witnessed by the compensation point of OCS concentration, where the soil flux is zero. For instance, the soil can change from an OCS source to sink when the atmospheric concentration of OCS increases. The balance between the uptake and production is strongly temperature dependent[17]. Both biotic and abiotic OCS consumption and production processes take place in soils. The biotic processes are affected by enzyme activity, which is affected by T, SWC, pH etc., while the abiotic processes are affected mainly by T. Light is also considered to be responsible for OCS production but the exact reactions involved remains unknown[29, 30]

2.2.1. OCS uptake mechanisms

OCS uptake is considered mainly enzymatic, governed by enzyme (e.g. CA) activity of soil microorganisms[31]. OCS consumption through other processes are negligible: hydrolysis at an uncatalyzed rate is rather small, and OCS destruction in the solid phase is only significant in very dry soils and in absence of other competitive adsorbents[32]. CA activity can be found not only in bacteria but also in actinomycetes and fungi.

CA activity is strongly correlated with geochemical abiotic and biotic characteristics of the ecosystem[33]. Besides the dependence on the ambient OCS concentration, the uptake of OCS by soils depends also on SWC (with maximum uptake rate between 10-15% by weight)[9]. Diest and Kesselmeier[21] suggest the uptake of OCS depends on the diffusivity dominated by water-filled pore space (WFPS) (Figure 2), which is also affected by soil temperature and soil type. In Figure 2, the deposition velocity V_d is used to describe the soil-atmosphere OCS exchange, where the V_d is calculated as the soil flux divided by atmospheric concentration of OCS ($V_d = F/C$). However, Kitz et al. [29] found that changing the SWC from 5% to 47% had no significant effect on the OCS flux, which is in conflict with some previous studies[21, 31].

These studies linked SWC primarily to OCS uptake, but Kitz et al [29] found that OCS emission prevailed. The lack of knowledge concerning microorganisms involved in the consumption of OCS make it difficult to predict the responses to water stress. Excessive soil moisture may lead to a lower biomass of microorganisms, mostly due to unfavorable oxygen conditions of aerobic microbes[34]. Drought can also disturb the microbes, as water is essential for maintaining the active state of enzymes[35]. The pH is also an important driver as it strongly influences microbial community composition, richness and diversity,

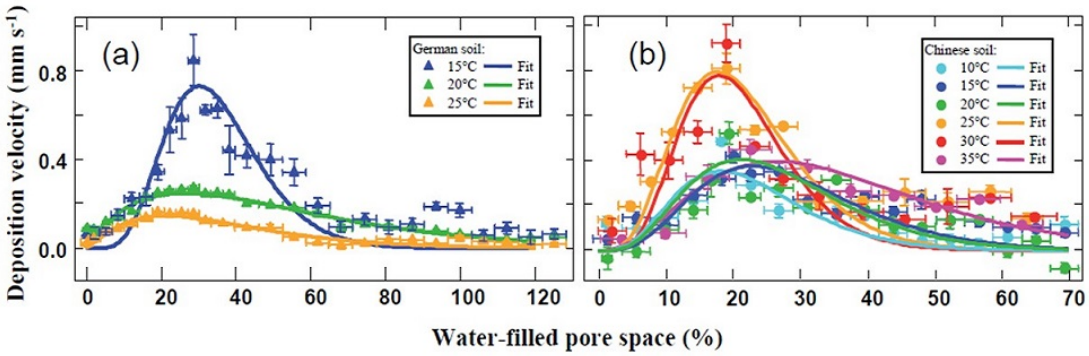

Figure 2: Deposition velocity (V_d; mms^{-1}; normalized uptake rate) in relation to WFPS (%) for two different soil samples at different temperature (a) the German arable soil; (b) the Chinese sandy soil[21], showing a strong dependence of soil OCS flux on soil moisture, soil temperature and soil type.

in addition to governing the speciation of CO_2 [36].

2.2.2. OCS production mechanisms

The mechanism behind the OCS production is considered to be abiotic thermal degradation and photo-degradation of soil organic matter. Sterilized soils exhibited a higher baseline of OCS emissions, suggesting that OCS production was abiotic and some of the OCS produced was consumed by in-situ microbes.[37]

Previous experiments[38, 30] concluded that the UV fraction of sunlight is responsible for abiotic OCS production, although the reactions involved are largely unknown. The OCS photochemical production rates in precipitation were found to be strongly dependent on sunlight intensity and independent of microbial activity as well as dissolved O_2[38].

Combining the uptake and production processes, there is disagreement on how the OCS soil fluxes change with T, as T interacts with other soil properties such as soil water thickness and soil organic matter. Kitz et al[29] found the OCS flux exhibited no optimum, but increased exponentially with rising temperature, in contrast to Kesselmeier et al[31]. However, this agrees with other studies[17, 37, 11]. Besides, a litter layer can be an important driver for these processes. Litter uptake in a Mediterranean oak woodland is found to important for surface OCS exchange[39].

3. Model description

In this thesis, the modeling effort of Sun et al.[19] and Ogée et al.[18] for OCS soil-atmosphere exchange are compared. Both models use diffusion-reaction equations (equation1), and resolve transport and source and sink terms in the soil. However, these two models are developed for different purposes: the Sun model is for a natural soil column, while the Ogée model is preliminary developed for interpretation of lab experiments. The Sun model resolves the diffusion process thus has the advantage of more realistic evaluation of OCS uptake, while the Ogée model provides a steady-state solution as the soil properties are fairly uniform in lab conditions.

Both models demonstrate good skill in simulating observed features of soil OCS exchange. For model validation, the Sun model uses the datasets from chamber measurements over an agricultural fields in the South Great Plains (SGP), and a Mediterranean oak woodland (SR), USA[17], while the Ogée model uses datasets from lab incubation data[21]. Both models can reproduce the observed transition from OCS sink to source at high soil temperature, and both models include parameterizations of the production and uptake terms.

To understand which drivers are important to the soil-atmosphere exchange of OCS, we first reproduced the depth-resolved, and time-resolved Sun model to test the sensitivity of OCS fluxes of different drivers. Then we reproduce the Ogée model for steady-state solutions under the same conditions. Therefore we start this chapter with the common parts of these two models, then introduce the different methods.

3.1. Parameterization of the processes

In this section, we describe the parameterization of diffusivity, dissolution, as well as that of the soil OCS uptake and production terms of equation from the Sun model and the Ogée model. Both models use the mass balance equation (Equation 1, chapter 2) to describe that the change of the OCS concentration (both dissolved and gas phase). The concentration of OCS with time in the soil is driven by the diffusion, production and uptake in the soil column. Further descriptions of the parameterization of each processes are in Table 1.

3.1.1. Diurnal variation of temperature

To investigate the effect of temperature on the OCS soil processes, we describe the change of temperature as a harmonic variation with time, dependent on both soil depth and time[40]:

$$T(z,t) = T_S + T_F \cdot \exp(-z/z_T) \cdot \sin(\omega t + \varphi - z/z_T), \tag{2}$$

where T_S is a yearly varying component; T_F is a daily varying component; φ is a phase constant to modify the time when max value appears, set as -0.5π to fix the maximum at 12 h on each day. Here we introduced the damping depth z_T, which is related to thermal properties of the soil and the frequency of variations as: $z_T = \sqrt{2\alpha_T/\omega}$, with $\omega = 7.27 \cdot 10^{-5}$ s^{-1}, and the soil thermal diffusivity $\alpha_T = 2.5 \cdot 10^{-7}$ m^2 s^{-1}. Hereby we set the T_S to be same as T_{ref} , and T_F as 10 K as an example of temperature profile (Figure 3).

Figure 3 displays the variation of the temperature in the soil column at 4 different depths in the soil column, respectively the depth of the first calculation grid (0.007 m),

the 10^{th} grid (0.05 m), the 20^{th} grid (0.37 m) and the last grid (1 m). Note that at z=1 m the temperature stays constant at T_S. The day starts at 0 h and the air temperature is set to reach the peak at 12 h (noon). At 24 h starts the new day.

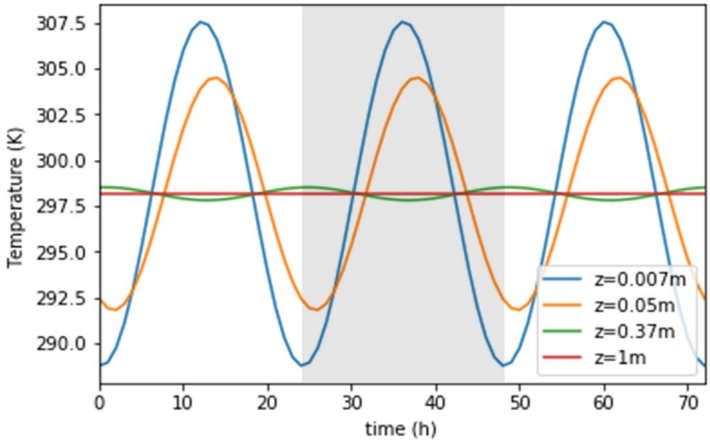

Figure 3: Harmonic variation of soil temperature of time in different layers for 3 days (72 h), with a daily variation ± 10 K of air temperature around $T_S = T_{ref}$= 298.15 K. The gray area marks the variations in one day.

3.1.2. Parameterization of diffusion and dissolution of OCS in the soil

The diffusivity of OCS in soil is affected by soil porosity (θ), water-filled pore space (θ_w/θ)) and temperature (T)[23]. In Table 1, we show the parameterization of the Sun model (undisturbed soil) and the Ogée model (repacked soil). Note that the Sun model assumes that there is no diffusion of dissolved OCS, thus the D_l is undefined.

Table 1: The parameterization of diffusivity in air D_a , diffusivity in water D_l, dissolution fraction k_H and uptake U and production P rate of OCS in the models. Note that the total diffusivity D including the diffusivity of OCS in air and in water $D = D_a + D_l \cdot k_H$. R is the gas constant (8.314 J mol^{-1} K^{-1}).

Parameterization	the Sun model	the Ogée model
D_a $(m^2\ s^{-1})$	$1.337 \cdot 10^{-5} \cdot {\theta_a}^2 (\frac{\theta_a}{\theta})^{\frac{3}{b}} (T/T_{ref})^{1.5}$	$1.27 \cdot 10^{-5} \cdot {\theta_a}^2 \cdot {\theta_a}^{1.5}/\theta \cdot (T/T_{ref})^{1.5}$
D_l $(m^2\ s^{-1})$	0	$1.94 \cdot 10^{-9} \cdot \theta_w \cdot {\theta_w}^{\frac{b}{3}}/\theta^{\frac{b}{3}} (T/T_0 - 1)^2$
$k_H(\backslash)$	$T \cdot \exp(\alpha + \frac{\beta}{T})$	$2.1 \cdot 10^{-4} [\frac{24900}{R} (\frac{1}{T} - \frac{1}{298.15})] \cdot R \cdot T$
U $(mol\ m^{-3}\ s^{-1})$	$-V_{Umax} \cdot \frac{k_H C}{K_M + k_H C} \cdot f(T) \cdot g(w)$	$f_{CA} \cdot k_{uncat} \cdot k_H \cdot \theta \cdot C \cdot \frac{x_{CA}(T)}{x_{CA}(T_{ref})}$
P $(mol\ m^{-3}\ s^{-1})$	$V_{SP,max} \cdot Q_{10}^{T-T_{ref}}$	$V_{SP,max} \gamma_P(E_h) \cdot Q_{10}^{T-T_{ref}}$

The diffusivity is described as an atmospheric diffusivity corrected by soil properties and temperature dependency. For solubility, we used the dimensionless Henry's law constant k_H to describe how much OCS can be dissolved in the soil water under certain temperatures. The k_H decreases with temperature for OCS (Figure 5(b)).

3.1.3. Parameterization of soil OCS uptake and production

We assume the uptake (U) and production (P) of OCS are separable terms: while production is represented as exponential function of temperature (Figure 5, 17 (a)), uptake is more complicated. In the Sun model, U is described as a maximum enzymatic

uptake rate V_{Umax} limited by enzyme activity's dependency on the temperature $f(T)$, the moisture $g(w)$, (Figure 4), and the availability of OCS (Michaelis–Menten equation, related with enzyme activity). K_M is the Michaelis contant for enzymatic OCS uptake by CA, 1.9 mol m^{-3}[41], which is equal to the substrate concentration at which the reaction rate is half its maximal value[42].

3.2. Model description of the column model

Following the equations of the Sun model[19] for surface OCS flux, we constructed the model step by step in Anaconda Spyder 3.1.4. We firstly only add diffusion in the model, and secondly added dissolution, and lastly the production and uptake term. For validation, We chose the SGP site (36.61° N, 97.49°W) data, which is one of the validation datasets of the Sun model.

3.2.1. Temperature and moisture dependency in the Sun model

Temperature and moisture dependent functions $f(T)$ and $g(w)$ of U are depicted in Figure 4 (site-specific for SGP). These functions are near bell shaped curves with a maximum around temperature of 281 K and water content of 0.20 m^3 m^{-3}. In Figure 4, for the moisture dependency on the right panel, when soil water content is 1 (soil pores filled with water), the fraction of the uptake rate over the maximum uptake rate is not zero, but of order 10^{-10}.

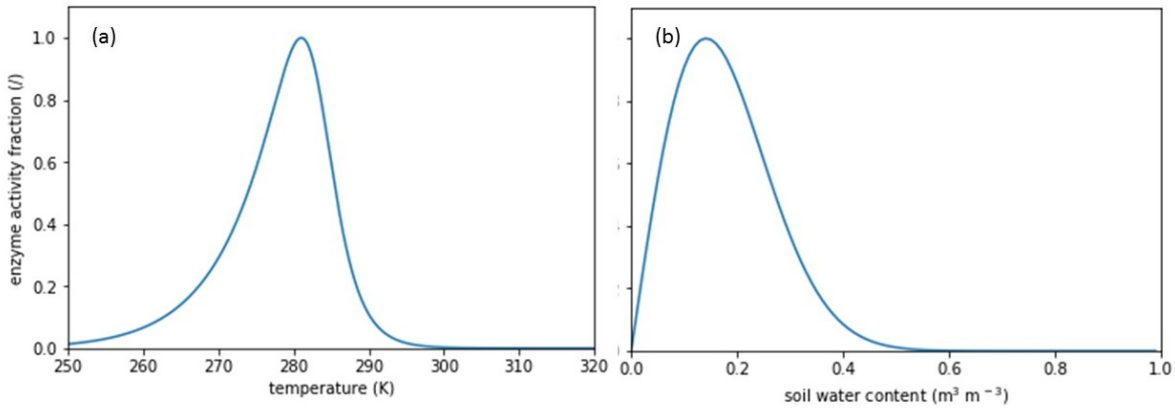

Figure 4: Dependence of normalized enzyme activity for OCS uptake of SGP site on (a) temperature and (b) moisture.[19]

3.2.2. Vertical discretization of the column model

Following the method of Sun et al[19], we discretized the partial differential equation (1) with the Crank-Nicolson method (CN)[43], which CN is by definition numerically stable and is often applied to diffusion problems. To solve the equation numerically, boundary conditions were set: the concentration at the top boundary equals the atmospheric concentration; and a zero-flux condition at the bottom boundary (1.09 m deep), assuming that is the lower boundary of the vadose zone. We used vertical grids to discretize the soil column, with similar equations as in the Community Land Model (CLM) 4.5 [44]. In that way the model could be integrated into global models in the future to simulate

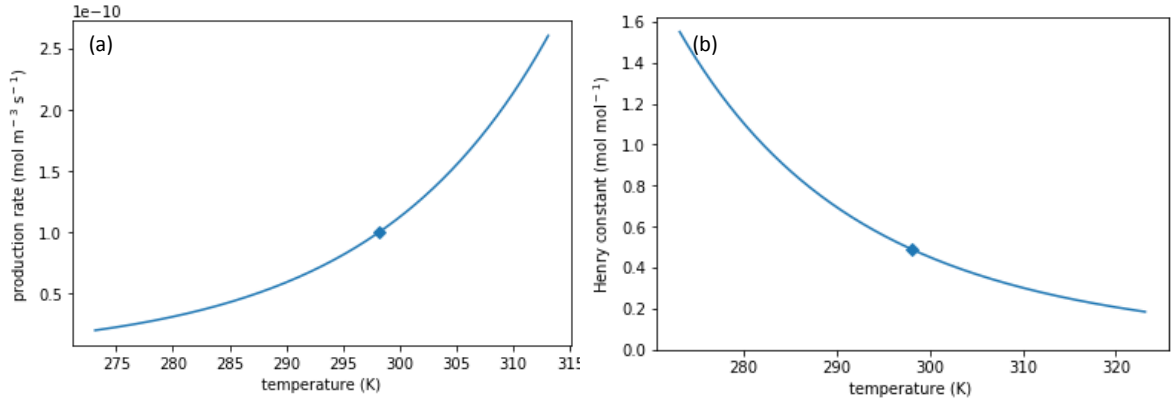

Figure 5: Temperature dependency of (a) OCS production rate of SGP site, with Q_{10} = 1.9[19] (b) Henry's law constant (T_{ref} 298.15 K marked with a diamond)

global fluxes. The depth of the computational nodes z_i (m) are defined with more nodes located near the surface.

$$z_i = \exp(0.2i - 5), i \in [0{,}25] \tag{3}$$

The total soil column depth till the last calculation node is 1 m. We used the face-centered control volumes as those give better evaluation of diffusive fluxes across interfaces, and the control volume depths are defined by differences of interfaces (Figure 6). The diffusive fluxes J_i were calculated from layer i-1 to layer i, with concentration C changes were calculated at each node through the soil column.

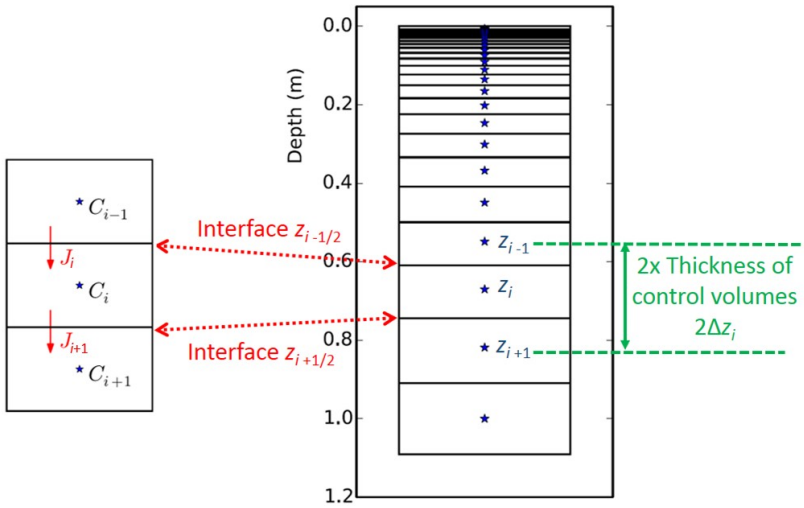

Figure 6: Vertical profile of computational nodes (blue stars), interface (red), control volume (green) depth with schematic illustration of OCS concentration(C) and diffusive fluxes (J) through vertical grids. After Sun et al.[19]

We discretized spatially equation 1 on defined nodes by integrating in each control volume. For the topmost layer, we assume the OCS surface fluxes can be calculated from an effective conductance G and a gaseous concentration gradient between the atmosphere

concentration C_a and the gaseous concentration C_0 in the first soil layer[45]:

$$J_{a\to 0} = -D_{a\to 0}\frac{C_0 - C_a}{z_0 - 0} = -G_{a\to 0}(C_0 - C_a) \tag{4}$$

where $D_{a\to 0}$ is the diffusivity from air to soil z_0, and more detail of diffusivity calculation will be given in section 3.3.1.

Throughout most of this thesis, we set the C_a as a constant value to 20.437 nmol m^{-3} ($2.0437{\cdot}10^{-8}$ mol m^{-3}). We got this value from converting OCS mixing ratio (500 ppt): first calculating the molar volume of air (T_{ref}, 1 atm) from the ideal gas law: $V = NRT/\mathrm{P}$, where N is moles of air (1 mol), R is the gas constant (8.314 J mol^{-1} K^{-1}), T is temperature (298.15 K), and P is air pressure (101325 Pa), and then we divided OCS mixing ratio by V.

3.2.3. Set-ups of the base run

We set the base run with diffusion as the only process involved. The diffusion processes started from no OCS in the soil column, and a constant C_a of 20.437 nmol m^{-3}. From t=0 we allowed OCS to diffuse from air into the soil. With temperature set to reference temperature (T_{ref}) 298.15 K, we eliminated the effect of temperature on diffusivity. The porosity of the whole column is set to be constant 0.5, and the diffusivity D inside the soil column is therefore also constant, while diffusivity of the interface is $2/(1/D - 1/D_a)$ (Table 1, D_a).

Table 2: Parameters of the base run

timesteps (s)	porosity $\theta(/)$	moisture θ_w $(/)$	air-filled porosity θ_a $(/)$	$T_{ref}(K)$
1	0.5	0.1	0.4	298.15

3.3. Model description of the steady-state model

With the same mass balance equation, the steady-state model or the Ogée model assumes isothermal and uniform through the soil column, and thus gives analytical solutions.

3.3.1. Steady-state solution of the Ogée model

We integrated the new Sun model for different homogeneous conditions at different temperatures until the surface flux reaches steady state, to compare it with the steady state solution for OCS soil flux from the Ogée model:

$$F = -\sqrt{k \cdot k_H \theta D} \cdot (C_a - \frac{z_1^2 P}{D}(1 - \exp(-z_{max}/z_1)), \tag{5}$$

where F is the soil flux (mol m^{-2} s^{-1}), positive for upwards flux (soil acts as an OCS source), k_H represents the dimensionless solubility of OCS in water (Table 1), C_a is the atmospheric concentration (mol m^{-3}), P is production rate (mol m^{-3} s^{-1}), D is the total diffusivity (m^2 s^{-1}), z_max is the soil column depth, and $z_1^2 = D/kk_H\theta$, while k, is the total hydrolysis rate (s^{-1}) (uncatalyzed rate enhanced by catalyzed factor f_{CA}, Table 1).

Compared to the Sun model, the Ogée model is attractive as it gives a relatively simple analytical solution with similar input variables, such as temperature, porosity, moisture, atmospheric concentration of OCS, etc.. Further, in Chapter 6 we implement the settings of the Ogée in the Sun model to reproduce the steady-state solutions.

4. Results: modeled OCS processes in the column model

First we set up the base run in which we only include the diffusion to test the time steps for eliminating fluctuations. Then we conduct sensitivity experiments for each OCS soil processes (diffusion, dissolution, production and uptake) separately to investigate which are the important drivers.

Figure 7 shows the results from the first simulations of the base run. The left panel shows the time evolution of the OCS flux at two different depths in the column: at a depth of 0.05 m (blue line) and at a depth of 0.37 m (orange line). First, it is observed that the fluxes approach zero after 6000 minutes (100 hours). This situation corresponds to a homogeneously filled soil column at a concentration that is equal to the atmospheric concentration. This is confirmed by the right panel. Fluxes are negative, representing the diffusion of OCS from air to the soil column.

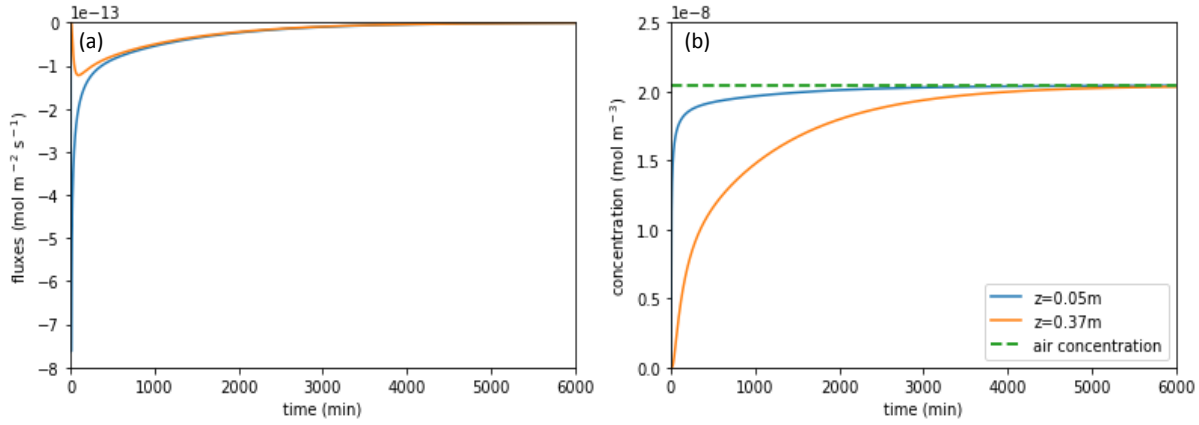

Figure 7: Diffusion process of the base run at different depths (10^{th} and 20^{th} grid) (a) fluxes change with time; (b) concentrations change with time. The green line in the right panel marks the air concentration of OCS.

4.1. Time steps for eliminating fluctuations

Although Crank-Nicolson method is unconditionally stable, oscillatory solutions (and even instability) are possible for larger time steps[46]. To avoid that, we test different time steps for discretization of base simulation (Figure 8). In addition, a larger time step saves calculation time, so it is needed to investigate the appropriate time step.

Before the diffusion starts, we assume there is no OCS in the whole soil column, which implies a huge gradient in the top soil layers. When a simulation is performed, we expect the soil pores to slowly fill with OCS, always with soil concentration decreasing with depth before they are completely filled (to reach the air concentration of OCS). Depending of the step size, this is not what is observed. To see clearly the fluctuation of the solutions, we zoomed in to the first 12 hours of the concentration-time figures as the concentration gradients are larger at the beginning of the diffusion process.

In Figure 8, when time step is large (e.g. (a) dt=1 h), the larger fluctuation is indeed happening in the layers closer to the surface, while the deeper layer has less oscillations. Similar case is for dt = 1 min (b), with a numerical instability in the layers near the

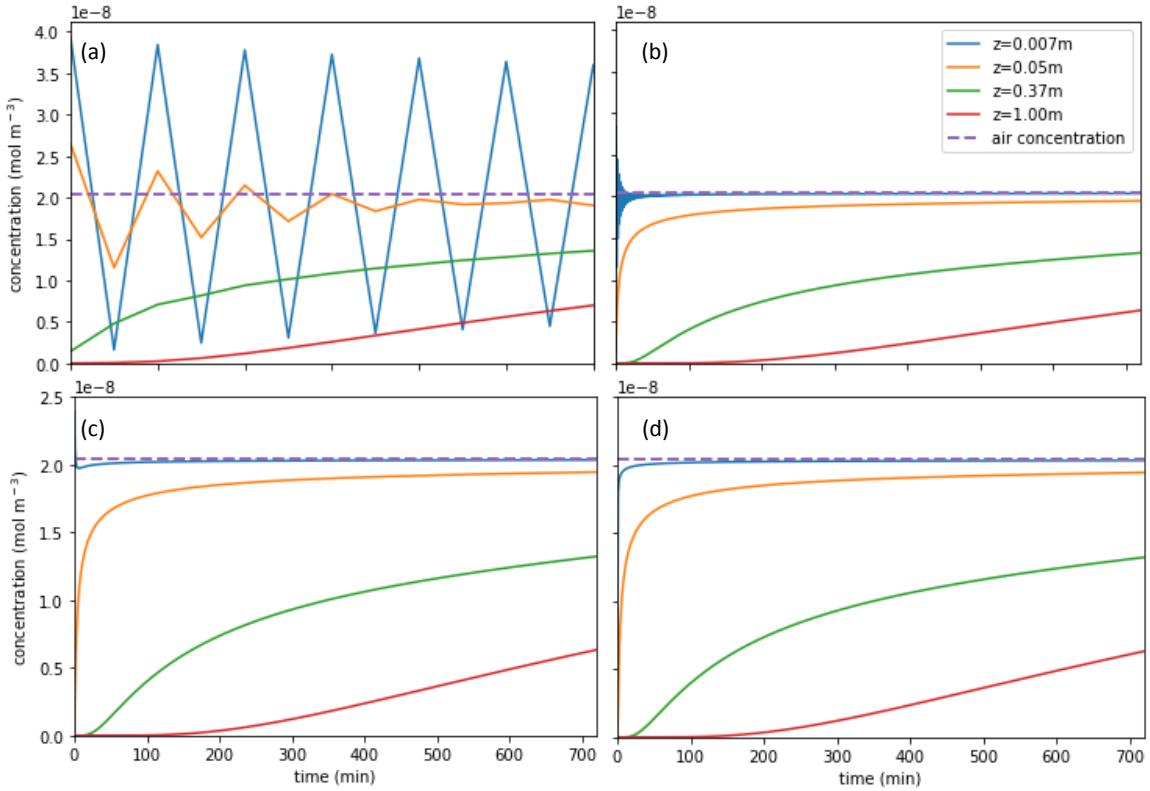

Figure 8: Evolution of the concentration with different discretization time steps (dt) of (a) 1 h; (b) 1 min; (c) 30 s; (d) 1 s, at 4 depth in the first 12 h diffusion process.

surface and at the beginning of the diffusion processes. When dt $<$ 1s (d), the numerical solutions of the differential equation are smooth, and the expected solution is obtained. Note that deep in the soil column the solutions are stable at already larger time steps. Moreover, when started with a filled column, a larger time step can be used without oscillation with only diffusion. However, considering adding sources and sinks in later tests will create large gradients, we selected time steps of 1 s for the model simulations in this study. The vertical profile of OCS changes with time, as OCS diffuses, the whole column gradually reaches air concentration. Figure 9 shows how the profiles of the OCS concentration evolve in time for the base simulation (see Table 2). It takes around 4 days to fill the entire 1 m deep pore space with OCS.

4.2. Drivers of OCS diffusion in the soil

In this section, we conduct sensitivity experiments varying the soil temperature and soil moisture to investigate the effects of porosity, temperature and moisture on OCS diffusion processes. We designed the sensitivity analysis based on the OCS concentration at 1 m depth (the lowest computation node) by comparing the corresponding time to reach 90% of the air concentration ($t_{0.9}$) (starting from an empty column). For the base run, $t_{0.9}$= 3031 min (around 2 days) (Figure 10, intersection of the orange line and the dash line).

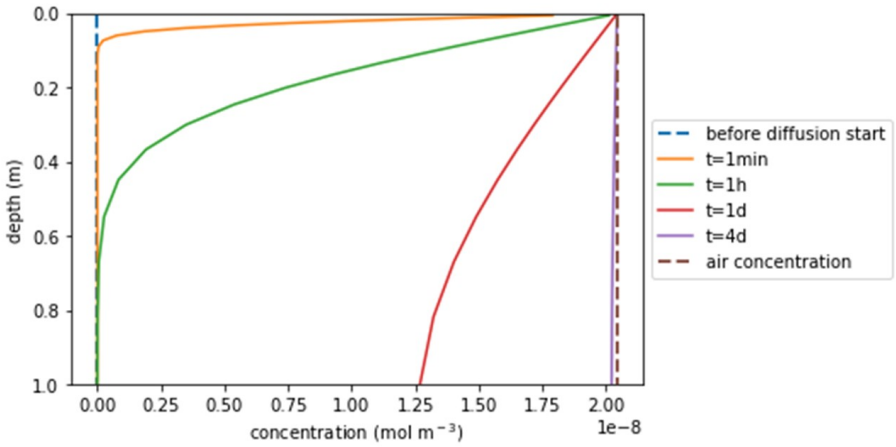

Figure 9: Time series of OCS concentration change after starting of diffusion process (from left to right) in soil pores.

4.2.1. Soil porosity

The influence of porosity on the diffusion process is large. Smaller porosity means less space for OCS to diffuse, which result in the smaller fluxes compared to the base run, and a larger $t_{0.9}$. We expect $t_{0.9}$ to decreases with increasing porosity, as the diffusion process is faster. By decreasing the soil porosity θ of base simulation with 0.1 to 0.6, the $t_{0.9}$ increased by 756 min (∼12 h). By increasing θ of base run by 0.1, $t_{0.9}$ decreased 503 min (∼8.4 h) (Figure 10(a)). We compared the base simulation with the porosity profile of SGP (0.6 in the top 2 cm, the rest the same as in the base simulation (Table 2)), the difference between these two $t_{0.9}$ values is in the order of 10 minutes, and thus negligible compared to $t_{0.9}$, which is in the order of days.

4.2.2. Soil temperature

We also tested the effect of temperature on the diffusion process in pore space, assuming no water in the soil column. The result shows the diffusion process is not very sensitive to a temperature change of 10 K. When decreasing T by 10 K from T_{ref}, the result shows a delay of $t_{0.9}$ by 159 min (∼2.6 h). An increase of 10 K decreased $t_{0.9}$ by 146 min (2.4 h) . When we set the daily temperature change of ±10 K around the T_{ref} with a harmonic variation with time (Figure 3), the $t_{0.9}$ remains nearly the same as the base run (3033 min) (Figure 10 (b)).

The influence of temperature on the diffusion process is therefore not very important compared with porosity as the difference in $t_{0.9}$ brought by the ± 10 K (Figure 11). For the diffusion process, the soil porosity is an important driver. As there was no water in the column for the above-mentioned simulations, the effects of water are discussed in 4.2.3.

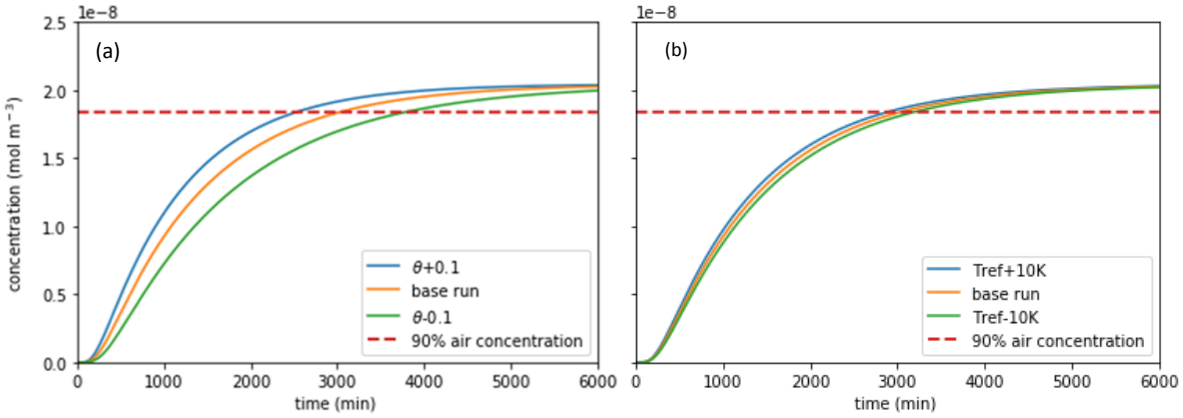

Figure 10: The concentration of OCS at 1 m depth in the soil column change with time, starting with an empty column and the atmospheric OCS diffuses into the column. The intersections with 90% atmospheric concentration mark the column as filled. Difference between the runs shows the effect of (a) 0.1 porosity difference; (b) 10 K temperature difference on the time for 1 m depth concentration reach 90% air concentration.

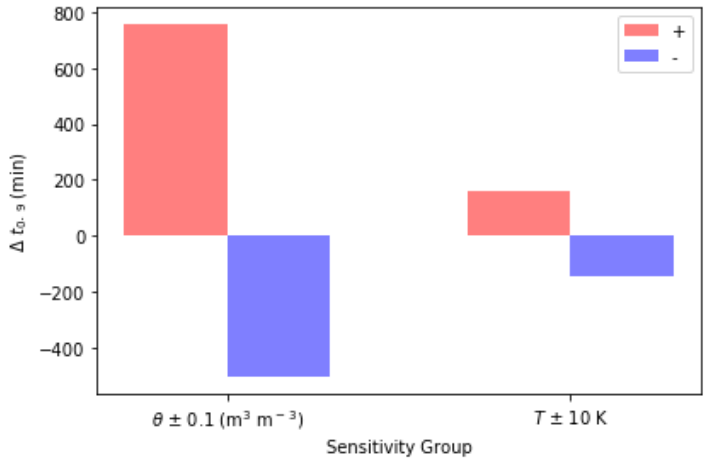

Figure 11: The effects of porosity change by 0.1 from 0.5, temperature change by 10 K from 298.15 K on the time for 1 m depth concentration reach 90% air concentration compared with base run (3031 min), red for plus and blue for minus.

4.2.3. Soil moisture

Soil moisture affects the soil-atmosphere exchange of OCS in two ways. Firstly, when the pore space is filled with water, diffusion will be slower (Table 1, D_a). Secondly, OCS is slightly soluble in water, and more water means more available OCS for uptake (Table 1, U). We consider dissolution as a sink and discuss that with the biotic uptake process in section 4.4.2.

We first set k_H as zero to eliminate the effect of dissolution of OCS. We then compared the $t_{0.9}$ with increasing WFPS. Results are plotted in Figure 12. With the increase of water in the soil column, the diffusion process slows down nearly exponentially. When the WFPS is 70 %, it takes nearly 14 d for the lowest grid's concentration to reach 90% of the air concentration. Thus, soil moisture is an important driver for the diffusion process.

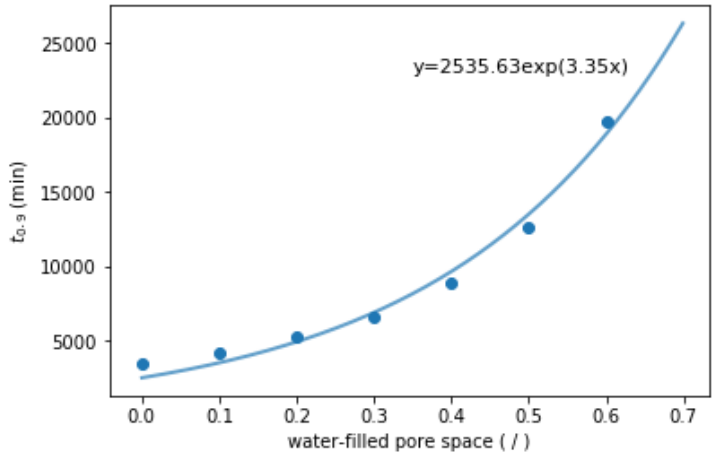

Figure 12: The effect of WFPS on the time for the 1 m depth concentration reach 90% air concentration, with total porosity of 0.5.

4.3. Drivers of OCS source in the soil

In the column model, the production mechanism of OCS in the soil is thermal degradation, and thus only related with soil temperature. This enables us to discuss the driver for the source without considering the availability of OCS in the soil. We will investigate the coupling of diffusion and the OCS production processes in section 4.3.1. Subsequently, we investigate the temperature dependency of production in 4.3.2. We use soil flux to describe the soil-atmosphere OCS exchange: positive values when the soil acts as an OCS source; negative values when the soil acts as sink.

4.3.1. Coupling of the source term

We checked the coupling of production in the column and diffusion by checking if the steady-state OCS flux at the soil surface equals to the integrated production. We added a source of OCS (10^{-10} mol m^{-3} s^{-1}) in the soil on top of the settings of the base run (Table 2). We checked two cases: adding a source to the whole column and to a certain layer.

First, we checked the steady-state profiles when adding the source in the whole column (Figure 13). At steady-state, flux profile is linear as expected, and a positive soil flux of $1.09{\cdot}10^{-10}$ mol m^{-2} s^{-1}, which is the integration of the flux over the whole column (1.09 m). The right-hand panel shows the time evolution of the surface flux. Again, a typical time scale of 6000 min is found for reaching steady state.

Second, we checked the fluxes and concentration profiles when adding the source only in the 10^{th} layer (0.045m to 0.055m). In this case, the steady state surface soil flux equals to the integration of source strength over the layer which is $0.010 \times 10^{-10} = 1.00 \cdot 10^{-12}$ mol m^{-2} s^{-1}, as expected. The column under the source was gradually filled, and the concentration there reaches steady state higher than air concentration (Figure 14(a)). For the concentration of the layers below the source, the closer it is to the source, the faster the steady state is reached, e.g. the z=0.37 m layer going faster than the z=1.00 m one (Figure 14(b)). This shows the transport of OCS from the source to deeper layer,

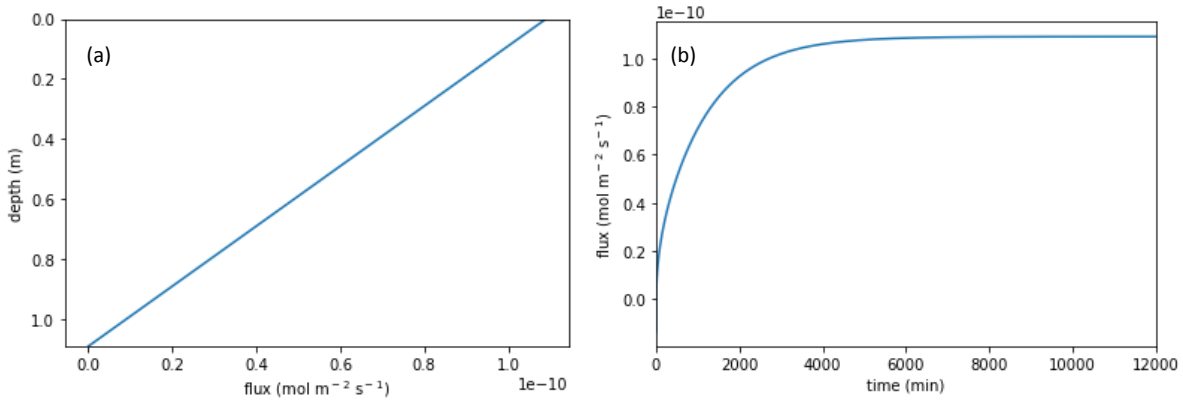

Figure 13: (a) Steady-state profiles using a constant OCS production rate of 10^{-10} mol m^{-3} s^{-1}in the soil column (b) time evolution of the surface OCS flux.

therefore the production term of the model performs properly.

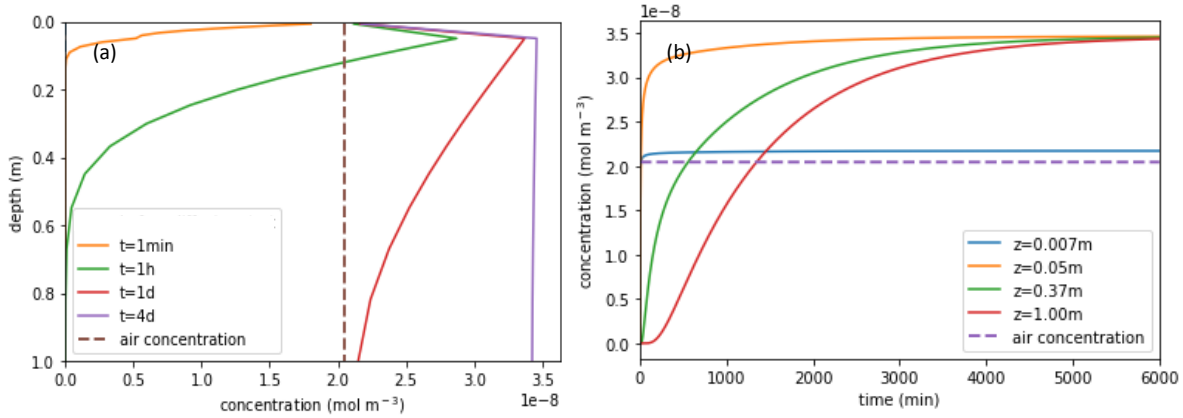

Figure 14: Added OCS source (10^{-10} mol m^{-3} s^{-1}) in the 10^{th} layer (0.045 m to 0.055 m), resulting in: (a) concentration vertical profile changes with time; (b) concentrations in different layers change with time

4.3.2. OCS Source strength and soil temperature

In our model, the OCS production rate increases exponentially with rising temperature (Table1, P), as only a thermal degradation source is considered. When the temperature changes from 273.15 K to 313.15 K, the OCS production rate increases roughly one order of magnitude, from 10^{-10} to 10^{-9} mol m^{-3} s^{-1}. We checked the change of production rate and soil fluxes when a diurnal cycle in the temperature is applied in the production and diffusion. In Figure 15, to show clearly the dynamics of the production, we only show the flux after 7 days of the simulation starts to the day 10, when steady state has been reached. The right-hand panel in Figure 15 displays the fluxes at different depths in the soil.

As the production rate increases exponentially with temperature, the change of production rate of +10 K and -10 K (the magnitude of temperature change in z=0.00 7 m layer) is not symmetric (Figure 15 (a)). The magnitude of the change in production rate with time is higher in the shallow layers than in deep layers, as the temperature diurnal

cycle is larger in the shallow layers (Figure 15).

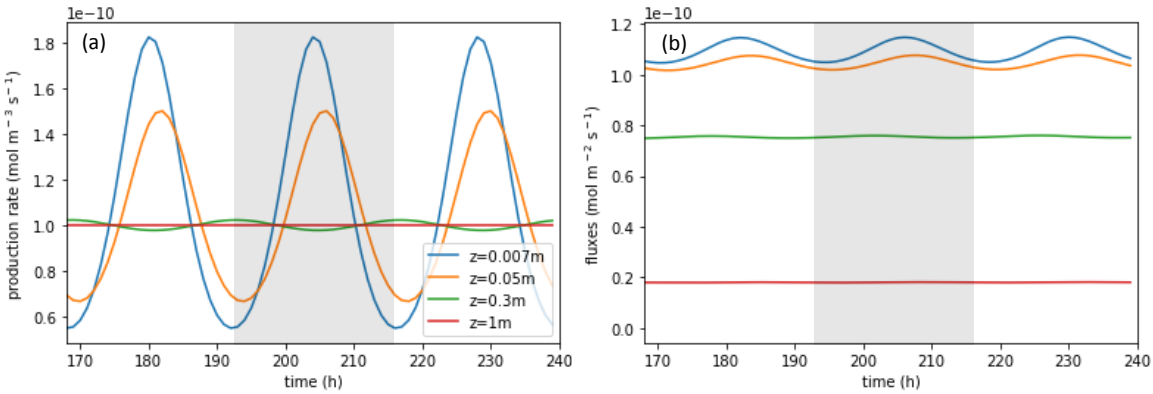

Figure 15: OCS production rates' dependency on a dynamic temperature (Figure 3) from day 7 to day 10, (a) production rate change with time; (b) OCS soil fluxes change with time. (Production rate is 10^{-10} mol m^{-3} s^{-1} at T_{ref} 298.15 K)

4.4. Drivers of OCS sink in the soil

We consider the dissolution and the enzymatic reaction (or uptake) of OCS together as OCS sink, and call it hydrolysis. The strength of the sink of OCS is thus related with soil temperature (also influencing the gas-liquid exchange), OCS concentration, and moisture (Table 1, U). First we first investigate the model's behavior to check if the sink term is coupled in the model. Second, we analyzed the sensitivity of the sink to the OCS ambient OCS concentration. Third, we checked the temperature dependency and moisture dependency of the sink strength. For better illustration of the sink, we chose the initial condition with a soil column filled with OCS at the atmospheric concentration.

4.4.1. Coupling of the sink term

Similar to section 4.3.1, we added a sink (Table 1, U) in the 10^{th} layer while setting the sink strength in other layers to 0 to check if the effect of uptake on concentration profile is as expected. With time progressing (from right to left in Figure 16), the concentrations in the layers below the sink reach a steady state which is less than atmospheric concentration C_a as expected.

We also validate the surface soil flux with the sink strength integration: the sink strength in the 10^{th} layer is -2.85·10^{-12} mol m^{-3} s^{-1}, and the thickness of the layer is 0.01 m, the soil flux is -2.85·10^{-14} mol m^{-2} s^{-1} as expected, so the uptake term is implemented correctly.

4.4.2. Ambient OCS concentration and the hydrolysis rate

The uptake of OCS depends on the OCS availability in the soil. The more OCS is available, the more OCS can be taken up (assuming there is enough enzyme CA in the soil). Although the saturation effect of enzyme activity of the Michaelis-Menten mechanism exists (section 3.1.2), due to the low concentration of OCS in the soil, V_{Umax} (corresponding to an uptake of uptake is of 0.12 mol m^{-3} s^{-1}, saturation of the enzyme (red dashed line in Figure 17(a)) will not be reached normally. Therefore, the dependency

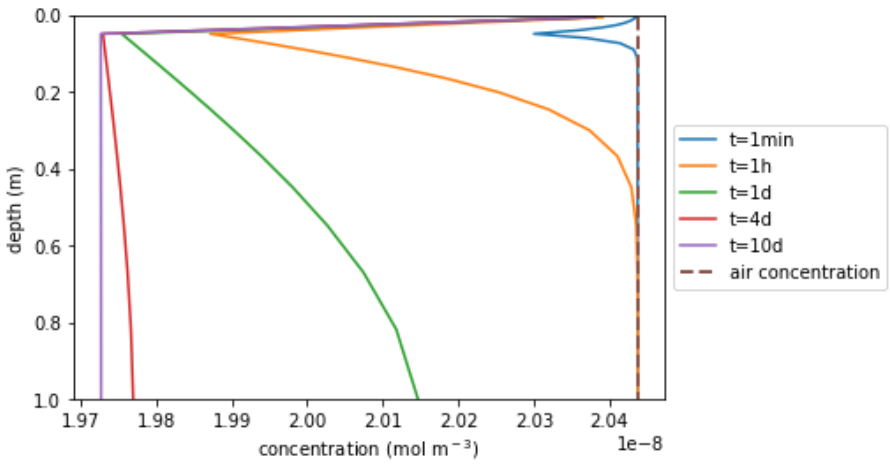

Figure 16: Concentration profile change with time (from right to left) when start with a filled column of air concentration and an OCS sink in the 10^{th} layer (0.045 m to 0.055 m deep in the soil). The sink strength is -2.85·10^{-12} mol m^{-3} s^{-1}.

of OCS uptake rate for the soil concentration is still in the linear zone (Figure 17(b)). As dissolution is also linearly correlated with ambient OCS concentration, the OCS hydrolysis rate is linearly correlated with ambient OCS concentration in the soil.

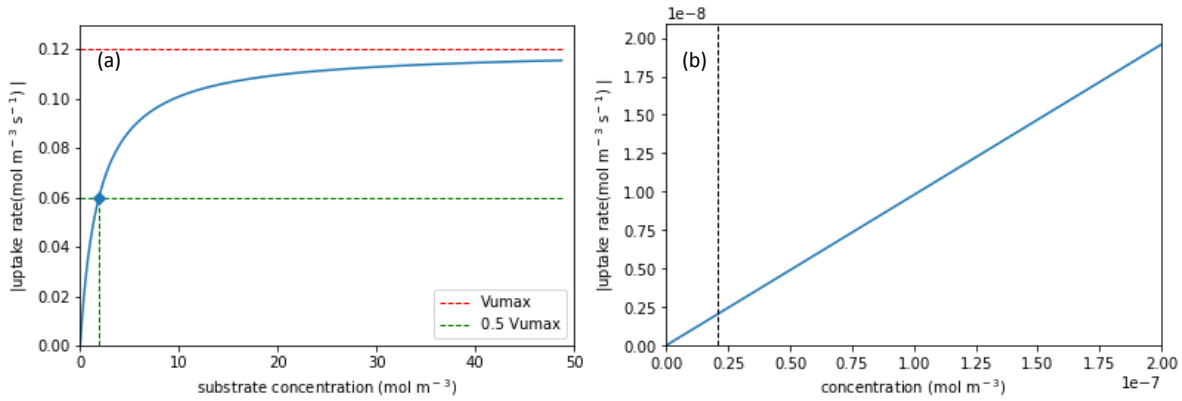

Figure 17: Dependency of uptake rate absolute value on (a) substrate (dissolved OCS) concentration (Michaelis constant 1.9 mol m^{-3} marked with a diamond) (b) zoom-in of a.(black dash line is the OCS air concentration), showing the linear relationship between uptake rate and concentration when concentration is in the range from zero to 10 times the OCS air concentration. Note the large difference in the x-scale in both figures.

4.4.3. Soil temperature & moisture and the hydrolysis rate

The enzyme CA's activity contributes to the uptake process through a pseudo-first order chemical reaction rate, which is influenced by both temperature and moisture. We performed tests on the effects of temperature T, as it influences the reaction rate as well as the enzyme activity. As moisture does not directly affect the reaction rate but the enzyme activity, we did not perform further tests with various WFPS.

Regarding the temperature, the hydrolysis rate of OCS in the soil depends on two factors: one is the k_H, which determines the substrate concentration that can be further

taken up by CA; the other is $f(T)$, the temperature dependency of CA activity. Temperature can enhance the uptake process within a certain range by enhancing enzyme activity. Even higher temperature causes enzyme to denaturate and lose its activity irreversibly. We have seen previously that a higher temperature accelerates the diffusion processes, and slows down the dissolution due to a smaller k_H (temperature dependency of k_H shown in Figure 5).

Similar to section 4.3.2, we first tested the (dynamical) temperature dependency of the uptake rate with a sink implemented in the whole column (we excluded the spin-up stage). As shown in Figure 18, the fluxes and the concentrations of OCS in different layers change with time, the OCS in deeper layers is totally consumed. Shallower layers display a dynamical uptake rate change with time (z=0.05 m). This is driven by temperature variations, mainly on the first-order uptake rate (see Figure 18(a)).

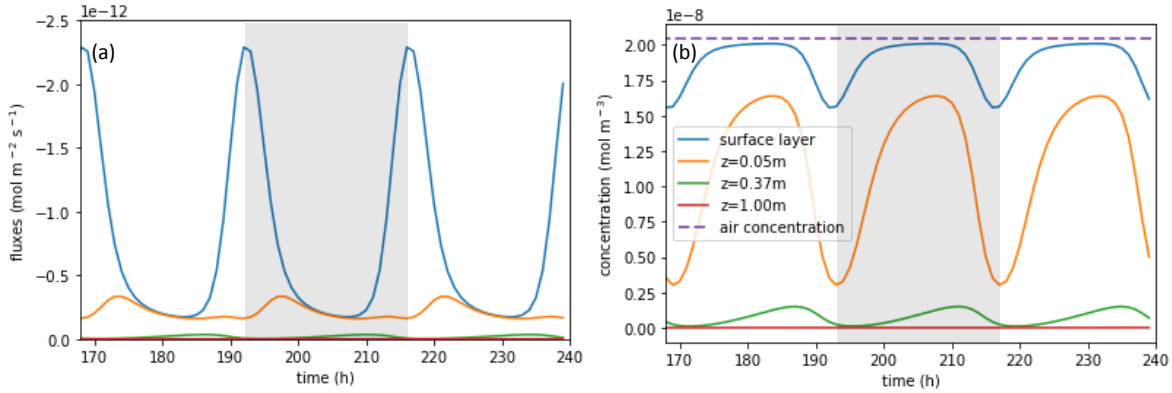

Figure 18: (a) Time evolution of the OCS flux at various depths in the soil in 3 days (72 h) after 7 days (starting from 168 h), with a temperature-dependent sink is applied in the entire soil layer (b) corresponding OCS concentrations in the soil. The gray area marks one diurnal cycle. Diurnal temperature change see Figure 3.

Regarding the role of soil moisture: soil water on one hand slows down the diffusion process limiting the OCS availability. On the other hand, similar to enzyme activity dependency on temperature, increasing WFPS first accelerates the uptake then suppresses it. The combined effects of temperature and moisture on relative uptake rate (1.0 means maximum uptake rate) are illustrated in Figure 19.

The uptake may be temperature limited or moisture limited. When T is above 298 K, the lines are flattened, showing a temperature limitation. When water content is above 0.5 m3 m^{-3}, the uptake rate is suppressed by too much moisture. As in this case, the rate of oxygen transfer becomes insufficient to meet the metabolic demands, the composting system becomes activity restricted, and eventually turns anaerobic. Also, too much water may result in clumping of substrate particles making further handling of the substrate difficult (Ray; Ward 2008). In our case with air temperature change ±10 K from 298 K, the high temperature becomes the limiting factor for uptake at the noon (at least close to the surface). For the water content, the observed value for SGP falls in the range of 0.05 to 0.45 m3 m^{-3}, and generally does not change very rapidly, so we consider temperature as the most important factor for dynamical change of the OCS soil uptake flux.

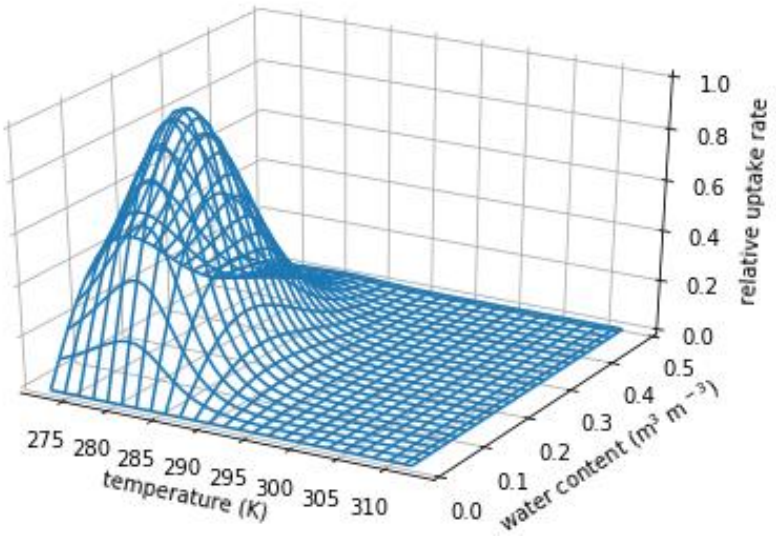

Figure 19: Modeling OCS relative uptake rate (i.e. the relative CA enzyme activity) in relation to temperature and moisture.

5. Soil OCS flux sensitivity to different drivers in the column model

After studying the production and uptake processes separately, we test the sensitivity of the soil flux on different drivers by combining these processes. Here we choose temperature, ambient OCS concentration, and the vertical distribution of the source and sink to study their effects on the transition of the soil from OCS sink to source (negative flux to positive flux) and vice versa. These drivers have different effects on the production and the hydrolysis: (1) a higher temperature enhances the production, and the uptake to some extent; (2) ambient OCS concentration determines the OCS availability (both from transport and production) for the uptake process; (3) uptake or production in the deeper soil layers may be overshadowed by production or uptake closer to the surface; and (4) transport thus far seems the limiting factor, since it takes in the order of days to exchange air between the soil and the atmosphere. Drivers like WFPS strongly influence the transport.

5.1. Soil temperature and the sink to source transition

To study the effects of temperature on the transition of soils from sink to source, we firstly checked if the model can reproduce typical soil OCS profiles at different temperatures; we secondly ran the model with a temperature range to investigate the trend of OCS flux change with temperature. The column is set to be homogeneous (Table 2,3).

We first checked the soil OCS concentration profile at steady state, T_{ref} (298.15 K), using an isothermal soil. In this case, the production rate is 10^{-10} mol m^{-3} s^{-1}, and the uptake rate is smaller, therefore the soil acts as a net source of OCS. At the steady state, the flux reaches $1.14{\cdot}10^{-11}$ mol m^{-2} s^{-1} (Figure 20(a)), and a steady-state concentration in the upper most layer of $4.36{\cdot}10^{-8}$ mol m^{-3}, i.e. higher than the air concentration (Figure 20(b)). We then decrease T by 10 K. At this T, the production rate is $5.26{\cdot}10^{-11}$ mol m^{-3} s^{-1}, while the uptake rate is higher than the production rate, so the soil acts as a net sink of $-2.05{\cdot}10^{-12}$ mol m^{-3} s^{-1}.Therefore the model can reproduce the observed temperature-dependent transition from source to sink[17, 19].

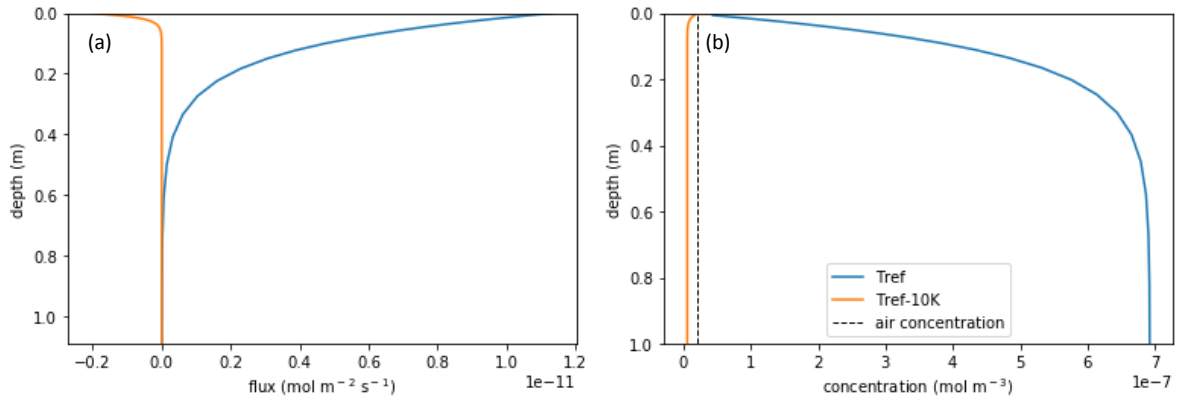

Figure 20: Simulated typical profiles of OCS (a) fluxes; (b) concentration, when the soil acts as a source or a sink at different temperatures. The orange lines represent $T = T_{ref} - 10$K (soil sink of OCS), while the blue ones correspond to $T = T_{ref}$ (soil source of OCS).

Table 3: The parameters of diffusivity in air D_a , diffusivity in water D_l, dissolution fraction k_H and uptake U and production P rate of OCS in the models. For the equations see Table 1. Note that the settings of the Ogée model are later used in the new Sun model.

Parameterization	the Sun model	the Ogée model
D_a $(m^2\ s^{-1})$	b=5.3	-
D_l $(m^2\ s^{-1})$	-	-
$k_H(\backslash)$	α=-20.00; β=4050.32	-
U $(mol\ m^{-3}\ s^{-1})$	V_{Umax} =0.12; K_M= 1.9 mol m^{-3}	f_{CA}=30 000
P $(mol\ m^{-3}\ s^{-1})$	$V_{SP,max} = 1 \cdot 10^{-10}; Q_{10} = 1.9$	$\gamma_P(E_h) = 1; Q_{10} = 3$

We then performed more simulations at different temperatures between 273.15 and 303.15 K to reproduce the transition of soil from OCS sink to source (Figure 21).

From the model output, we observe that with an increase of T, the soil firstly acts as an OCS sink. It then reaches the optimum around the optimum temperature for enzyme activity (281 K). With decrease of enzyme activity and an increase of production after 281 K, the soil gradually becomes an OCS source. When the temperature gets higher than 295 K, the OCS soil flux follows an exponential growth, where the points are more scattered. This also agrees with the trend that the enzymatic uptake is suppressed by high temperature (above 295 K, Figure 19) and production increases exponentially (Figure 5 (a)). In this temperature-range, the OCS soil flux is production dominant. At the temperature near to the transition, the steady-state soil flux exhibits a linear response to the temperature, with two processes canceling each other out, and a surface flux changing linearly with temperature (Figure 21, the zoom-in figure).

Ogée et al[18] used a relatively higher optimum temperature of enzyme activity than that used by Sun et al[19], which has its maximum at relatively low temperatures (280.95 K = 7.8 °C). Additionally, given the temperature range of SGP site (averagely higher than 20 °C observed period)[17], the optimum temperature of enzyme is not expected to be as low as 7.8 °C. Therefore we performed similar tests with a higher optimum temperature, When moving up the optimum temperature for CA activity from 280.95 K to 298.15 K, we observe a change of both the maximum uptake rate and the transition temperature (Figure 22, modified Sun). When the temperature dependency of production stays the

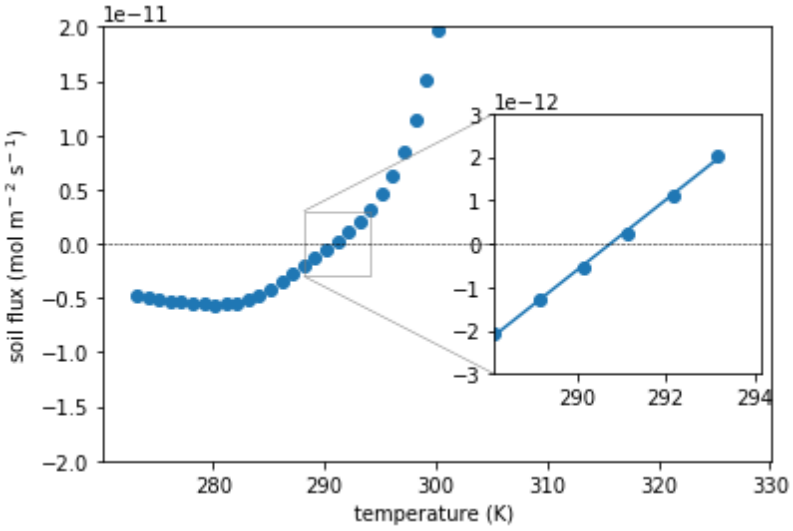

Figure 21: Variability of OCS soil fluxes related to temperature (between 273.15 and 303.15 K) with a zoom-in to the linear zone near the transition from source to sink ($y = 7 \cdot 10^{-13} x \check{} 2 \cdot 10^{-10}, R^2 = 0.99$). The horizontal dashed line marks the zero flux. Note that every point is the steady-state soil OCS flux at this temperature.

same, the influence of the modification on the total soil OCS flux is mainly in the uptake part (negative flux). For production dominant fluxes, the shape stays the same, while a shift of the transition temperature is smaller than the shift of optimum temperature for CA activity. This is because of the exponential growth of production rate with temperature. For the same reason, the maximum in the uptake flux becomes smaller after the change, since the uptake at the optimal temperature coincides with higher production.

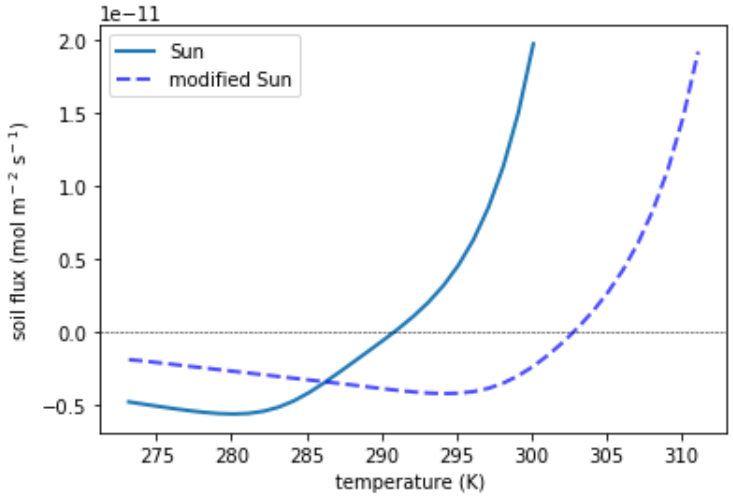

Figure 22: Comparison of the variability of OCS soil fluxes related to temperature with optimum temperature for enzymatic uptake of OCS is of 280.95 K (Sun) and of 298.15 K (modified Sun).The horizontal dashed line marks the zero flux.

To sum up, the temperature is an important driver for the soil flux, both for the direction and the magnitude, especially for the upper soil layers, where the temperatures change more rapidly than that in the deeper layers. As the enzymatic hydrolysis rate is also dependent on the moisture, with also a bell-shape curve similar to the temperature,

the effects of moisture on the soil OCS flux are not included here, more detail see Appendix A.2.

5.2. Compensation concentration and the sink to source transition

The exchange rate of OCS and its dominant direction are dependent on ambient OCS concentration, and there is a so-called compensation concentration (i.e. the OCS concentration at which the net flux is zero)[31]. Generally the compensation concentration is below the atmospheric concentration, C_a ($\sim 0.2 \cdot 10^{-7}$ mol m^{-3}), thus the soil acts mostly as a sink under natural conditions. We perform simulations for flux sensitivity on ambient OCS concentration of the Sun model, and the compensation concentration is the intersection of the flux line with the zero flux dash line in Figure 23.

We expect a linear relationship and the results confirm the linear response of hydrolysis rate to C_a within the concentration range of our tests. As the production term is independent of the OCS concentration in the soil, at certain T, the total flux of the soil is dependent on hydrolysis rate. We also observe that a higher T favors the production thus results in higher compensation concentration. The change in the slope for different temperature, showing the suppression of enzyme activity at higher temperature: when T 10 K higher than the T_{ref}, the slope becomes $-4 \cdot 10^{-7}$, which is smaller than $-1.69 \cdot 10^{-5}$ at 298.15 K (Figure 23). Vice versa, at $T_{ref} - 10K$, the slope is 10^{-4}, steeper than that at T_{ref}.

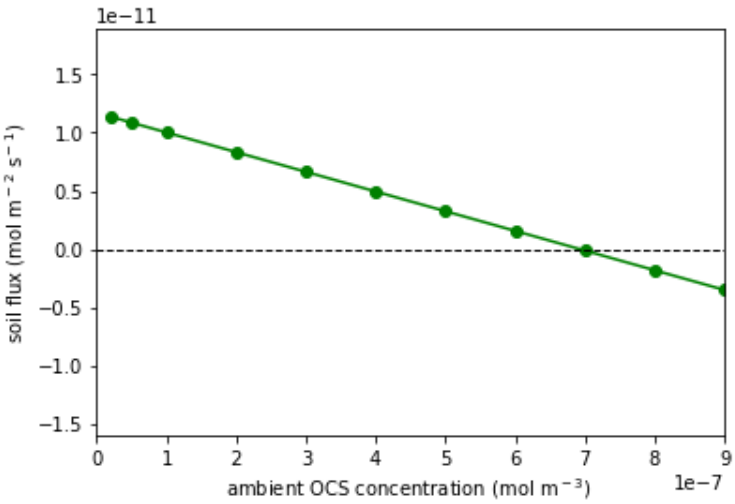

Figure 23: The relationship between ambient concentration and soil OCS flux in the Sun model, when temperature is 298.15 K in the whole soil column. The black dash line marks the zero flux, at which is the compensation concentration. $y = -1.69 \cdot 10^{-5} \cdot x + 1.17 \cdot 10^{-11}$, with $R^2 = 0.99$

In Figure 23, the compensation concentration at 298.15 K is higher than the C_a, it shows that in this situation, the soil can only act as a source at C_a. This agrees with the fact that the enzyme activity is highly suppressed, therefore the emission is the dominant process (Figure 20, blue lines). When T is lower, the compensation concentration is lower, and vice versa. A similar test is done with the Ogée model, and the results also follow the same pattern, see Figure A.31.

The compensation concentration is a changeable value, mostly due to the change of enzyme activity. Therefore the drivers that influence the enzyme activity affects the compensation concentration. The relationship between the ambient OCS concentration and soil flux is linear at steady state, as the available OCS decides the how much the soil can take up.

6. Reproduce the steady-state solution with the column model

As mentioned in section 3.2 & 3.3, the Sun model (or the depth-resolved column model)[19] and the Ogée model (or the steady-state analytical solution model)[18] do not have the same output as the uptake rates are described differently. Therefore, we aimed to use the column model to reproduce the steady-state outputs by implement the same drivers and processes of the Ogée model in the Sun model, and we refer to it as the "new Sun model".

6.1. Set-up of the new Sun model

With the new Sun model, we resolved the Ogée model (Equation 1) explicitly in the Sun column model. Firstly we built the Ogée model and validate the model to see if it produces the same result as in the literature[18]. Secondly, we based the soil properties on the SGP site, and set the soil column as homogeneous and isothermal (Table 2), and sources and sinks in all the layers of the soil. Thirdly, we changed the modified Sun model with set-ups from the Ogée model and ran this new Sun model until steady state for soil OCS flux. Lastly we compared the output from the new Sun model with Ogée model output. For the new Sun model, a time step of 0.5 s is needed for avoiding numerical instabilities.

The equations and parameters are described in Table 1& 3, the Ogée model column. The typical enzymatic enhancement factor of hydrolysis f_{CA} ranges between 21 600 and 336 000, with a median value at 66 000[18], while f_{CA} is set to be 30 000 in our new model. This smaller f_{CA} reflects a smaller uptake rate in the Sun model compared to the Ogée model. For instance, at T_{ref} the hydrolysis rate (calculated as uptake rate/ concentration) from the modified Sun model is 0.032 s^{-1}. This means that it takes 31.25 s for the OCS uptake. Note that this is much faster than the transport time scale in section 4.2 ($\sim$2 d).

6.2. Comparison of the outputs from the new Sun model and from the Ogée model

The new Sun model and the Ogée model are set to have the same production rate, with Q_{10} =3.0[47], and hydrolysis rate of OCS (Figure 24(a)). We compared the steady-state soil OCS flux from these two model under with changing temperatures, and the outputs show good agreements between these two models (Figure 24(b)).

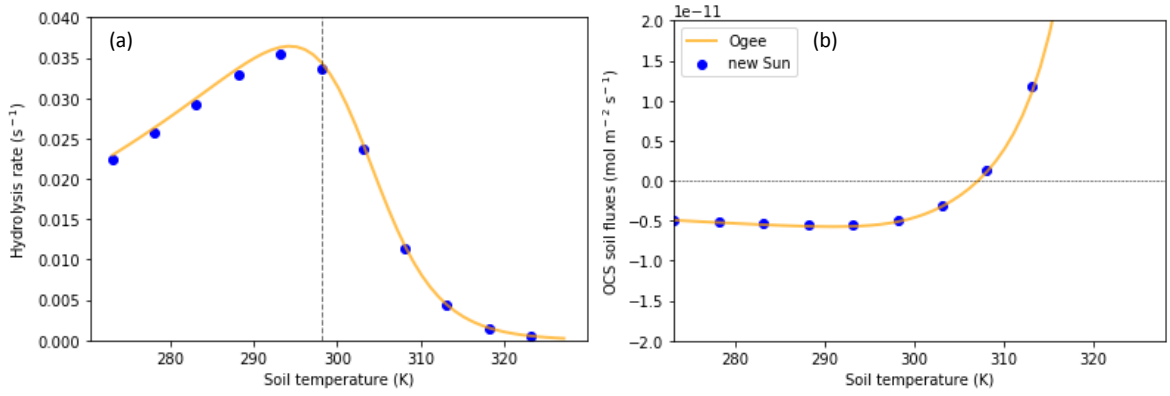

Figure 24: Comparison of temperature dependency of (a) the OCS hydrolysis rate (s^{-1}); (b) the soil OCS flux from the new Sun model and the Ogée model.

Now that we can reproduce the steady-state solutions with the column model, we can test the non-steady-state situations in the new Sun model to investigate how large is the difference between them.

6.2.1. Comparison of the responses of the OCS fluxes to the dynamical temperature

We start with the temperature dependency: as the temperature in the steady-state solution remains constant throughout the column, while the diurnal temperature change in the column model not only changes with time, but also changes with depth. Therefore we conduct simulations with diurnal temperature change (see Figure 3) to investigate how large is the difference between the steady-state solution and the column model output, which is not necessarily always at steady-state. We also compare the output of the column model with diurnal temperature change only with time not with depth: the column has the same temperate as the temperature at the first grid (z = 0.007 m, Equation 3).

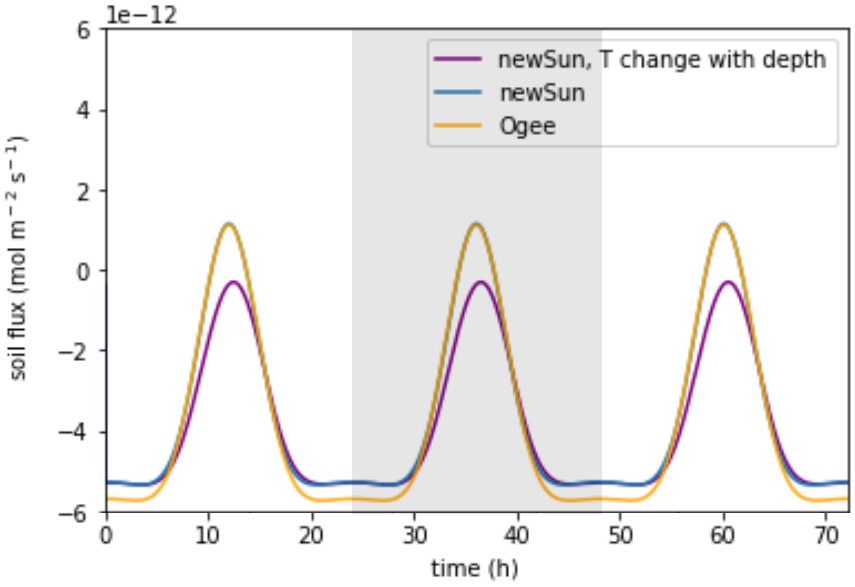

Figure 25: Comparison of flux change with dynamical temperature in the new Sun and the Ogée model in 3 d. The blue line represents the same temperature in the whole column, while the purple line represents the temperature change with depth (Figure 3). The gray area marks one diurnal cycle.

From the difference between the fluxes from the column model and the steady-state solution (Figure 25), the fluxes in the column model do not reach steady state immediately. The differences between the two models (orange and blue) are especially visible at the lower parts of the graph when it is uptake dominant. However, the blue and orange lines are almost overlapping when it is production dominant, although the difference is 0.03 pmol m^{-2} s^{-1}. Additionally, when the soil temperature changes with the depth, there is a delay in the fluxes' response of temperature (the purple curve). Thus if we apply directly the steady-state solution in a field condition, there will be an overestimation from the steady-state solution (the Ogée model) in uptake dominant situation, while an underestimation in production dominant situation. Therefore the column model has the advantage of time-resolving that could reproduce the field situation more realistically. Moreover, there is argument that as CA activity is high enough, OCS supply rather than the CA content and activity is the limiting factor[12]. This also agrees with other studies

that consider diffusivity play a major role in the exchange of OCS between soils and the atmosphere[21]. Our results also supports this argument as the difference of the temperature responses between the steady-state solution and the column model is caused by the transport.

6.2.2. OCS soil fluxes' responses to the temperature change after steady-state

As mentioned above that the flux in the column model has a delay of response of temperature if compared with the steady-state flux, we conduct tests to see how long does the column take to reach a new steady-state. We set the temperature in the soil change with depth but not with time, and after 60 min, we increase the temperatures in the whole column (Figure 26(a)). In Figure 26(b), we show the soil OCS fluxes change with time in two layers. While the deeper layer reaches the new steady-state in less than 5 min, the surface flux reaches the new steady-state around 10 min. This quick adaption to the temperature change also agrees with the small difference between the steady-state solutions and the column model in 25. Also, the magnitudes of changes are larger in the surface layer than in the deeper layer. Therefore, it is possible to correct for this delay of flux's response to the temperature change in the steady-state solution model. However this is not done in this thesis.

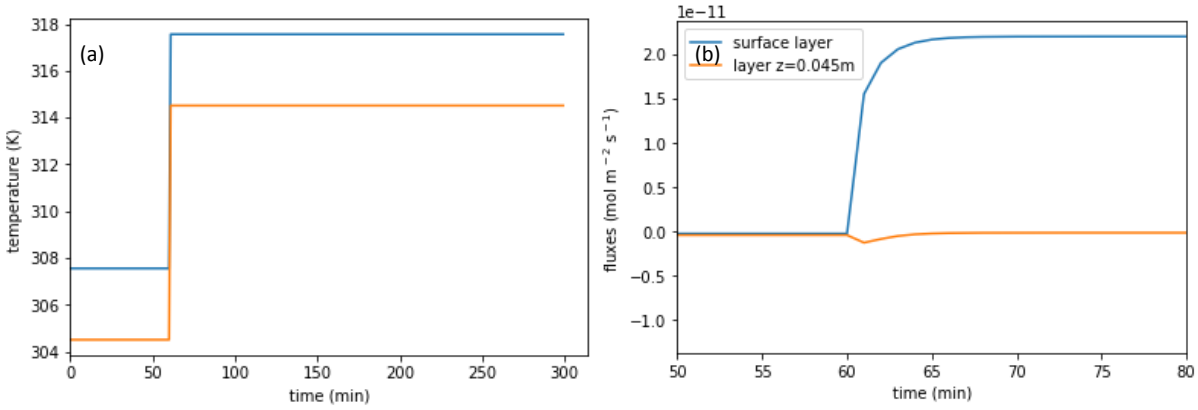

Figure 26: The effects of a change of temperature of 10 K at 60 min after soil OCS flux reaches steady-state. (a) temperature change with time; (b) zoom-in of the flux change with time in two different layers.

As the vertical profile of OCS sources and sinks will affect the OCS soil flux, while deeper sources and sinks have less influences on the surface fluxes. We carried out sensitivity analysis on added deeper sources in the following section.

6.3. Vertical profile of source and sink

So far most of the above-mentioned experiments are in a homogeneous soil column, where uptake and emission of OCS take place in the whole column. As the temperature variation is more dynamical in the shallower soil layers, and it takes longer for OCS in the deeper layers to transport to the soil surface, we expect that the shallower soil layers are more influential for the soil OCS flux. From steady state flux profiles in simulations with both OCS sources and sinks active (Figure 20(a)), the fluxes below 0.6 m is almost zero, thus the influence on the surface flux is mainly from layer above.

For the uptake process of OCS, microbes (containing CA) are typically most numerous in surface layers that are rich in organic material or in the rhizosphere where plant roots release sugars, amino acids and other organic compounds[34]. This indicates that more biotic uptake of OCS happens in the upper layers of the soil. For lab experiments, the samples were mostly taken from top 5 cm soil[48, 21], which is different with others using 10 cm[47]. The vertical profile of OCS sources and sinks are therefore important. For instance, experiments of responses of soil enzyme activity to flood found that the responses were larger at 10-20 cm than in the deeper soil layers . General decreases in biomass and reduced response of microbial markers were observed with increased sampling depth[34].

Knowing that the uptake of OCS is most influential in the upper layers of the soil, we aimed at testing the influence on the surface flux by a deeper OCS source. One limitation is that we do not know the OCS concentration in the deeper layers in the soil. Therefore we test the new Sun model with implementing sources in the deeper soil layers to see the response of soil OCS fluxes. Note that these experiments are not possible with the Ogée model.

6.3.1. Effects of an extra deep OCS source in the soil

Firstly we set the whole column in the new Sun model with $T = T_{ref}$. Then we multiply the source by 10 (10^{-9} mol m^{-3} s^{-1}) in different layers. Results are shown in Figure 27. While the concentration profile changes in the soil column (left panel), however at steady state, the soil OCS flux almost remains unchanged. Only when the source is augmented above 5 cm, the steady state soil OCS flux gets less negative, but the magnitude is rather small (right panel). The result shows that the hydrolysis is quick enough to take up the OCS before it reaches the soil surface, therefore the deeper source does not have a large effect on surface OCS flux. Of course, this results depends on the relative magnitude of sources and sinks. In this particular case, uptake of OCS clearly dominates.

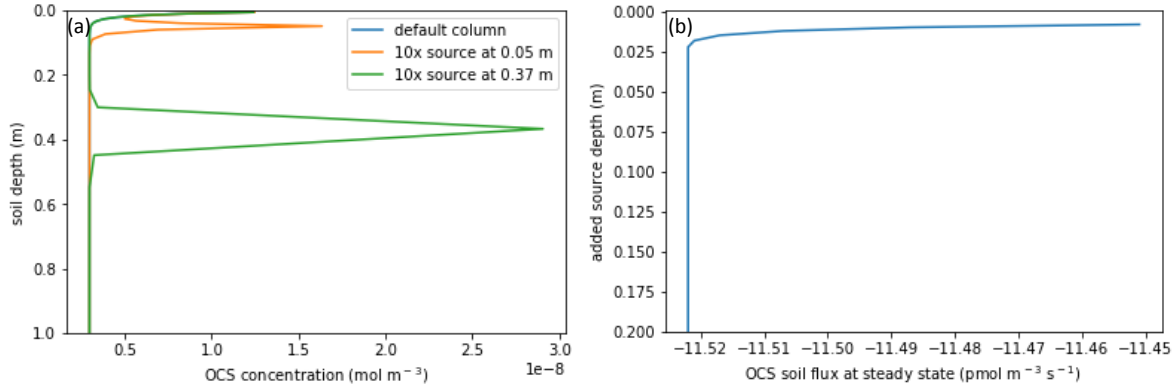

Figure 27: OCS steady state with added 10x (10^{-9} mol m^{-3} s^{-1}) sources at (a) two different depth, concentration profile; (b) added sources at different depth respectiviey, a zoom-in to the upper 0.2 m, showing the steady-state surface OCS fluxes at different depths of the added 10x source. Note that these two figures have different scales in both axis.

7. Discussion

In this thesis we were able to reproduce the some specific features of the soil OCS flux. The identification of important drivers for soil OCS flux with a column model provides information for further upscaling of OCS modeling. The model we built is process-based and therefore can be extrapolated to different sites. We were able to reproduce the steady-state model outputs with the column model, and tested for non-steady-state situations. However there are limitations, for instance we did not test the model with further datasets but only with the same datasets were used to build to model. However, the used SGP datasets are important as there are obvious production and uptake flux observed.

For the temperature dependency of enzyme activity, we consider that a higher temperature increases enzyme activity to a certain point, and after that the enzyme denatures, and loses activity irreversibly. The Sun model has applied recent enzyme kinetic modeling, which is based on the idea of a reversible equilibrium between an active and inactive form of the enzyme, and of a time dependent inactivation[49, 50]. However, in the Sun model, the optimum temperature for CA is relatively low (∼281 K, see Figure 4), for a site at which the observed temperature ranging between 278 K and 320 K[17]. This optimum temperature seems unrealistic. This might be related with enzymatic production of OCS in the soil, which shifts the optimum temperature of the total uptake rate (enzymatic uptake rate - enzymatic production rate) to lower temperatures.

CA is known to be one of the fastest enzymes, with a catalyzed rate k_{cat} up to 106 (s^{-1})[51]. In our model, the k_{cat} value is around 10^{-2}, which is relatively small compared to other CA studies. It is closer to the k_{cat} of nitrogenase, another enzyme that can catalyze the OCS hydrolysis[41]. This might imply that there are more enzymes responsible for the site of SGP, or the SGP site is not optimal for the CA. The Ogée model does not account for the moisture dependency of enzyme activity, and adding such a description can be helpful for interpreting field data. Another point that needs further investigation is that we did not take into account of changing redox potential and pH of the soil, but set it as constant terms to make the models comparable.

Using the Sun model, we can easily derive a time-dependent soil concentration profile. With OCS production in deeper layers, the concentration of OCS gets very large in the deeper layers (Figure 20, blue line). However, due to lack of measurement in the deep soil, the predicted large concentration is not yet validated.

There are other processes that might influence the soil OCS fluxes that not included in this model. For instance, neglecting the production of OCS by photo-degradation might be related with the underestimation high production rate at high temperature of SGP. Also, other reactions producing OCS such as CO with $MgSO_4$ with the minerals are not yet considered[52]. Except for microorganisms, there might be effects of other animals living in the soil on the soil OCS fluxes to be considered.

Moreover, the OCS mixing ratio is not always a constant of 500 ppt in the atmosphere as set in most of our simulations, and this affects the OCS availability. There are observed OCS mole fraction as high as 3008 ppt[48] and in soils below active vegetation the OCS mixing ratio can drop markedly. Therefore, it is important to have measurements of ambient OCS mixing ratios for soil flux estimation. Moreover, we did not include advection,

which might have a large influence on the OCS transport in the soil, thus influence the availability of OCS for uptake.

8. Conclusions

The main aim of this thesis was to investigate which are the important drivers for OCS soil flux especially for later upscaling. By firstly reproducing existing column and steady-state models of OCS soil fluxes, we conducted sensitivity analysis of these drivers.Temperature, moisture, and ambient OCS concentration and diffusivity are the important drivers for soil-atmosphere exchange of OCS. Under normal conditions, the uptake rate of OCS is linearly related to the ambient OCS concentration, and soil uptake can be described by a first order loss process. Temperature is the most important factor for reproducing the soil OCS flux as it varies fast, and both the uptake and emission of OCS are sensitive to it. At lower temperature, the soil flux is uptake dominant. At higher temperature the enzyme activity is suppressed, the emission of OCS from thermal-degradation dominates. When both OCS production and uptake are coexisting in a soil layer, a condition that is normally met, the upper soil layers are dominant in the soil-atmosphere exchange processes. Accounting for the transport of OCS with time is important for simulate the OCS flux observations, especially for upscaling, as the soil is not always at a steady-state. Correcting for the transport in a steady-state model to reduce the computational costs from the time-resolved and depth-resolved model can be an option for upscaling.

9. Recommendations

It is needed to investigate more soil types to allow modeling of OSC soil-atmosphere exchange on a global scale. The concentration measurement in deeper layer of the soil, especially for the OCS emission sites are helpful for learning more the soil OCS processes, specifically about the processes that drive OCS production (biotic of abiotic).

For the biological drivers, we need more lab research on both the enzymes or microbes, as there are more enzymes than just CA that is catalyzing the hydrolysis of OCS. Linking soil respiration rate with the activity of the soil microbes thus with the enzymatic uptake rate of OCS can be a useful tool.

For further modeling work, including the effects of stems, roots, and litter layers on OCS processes is recommended, especially the litter layers as the changes of the conditions are the largest there. Also, the OCS production by photo-degradation can be implemented in future work. Other drivers such as redox potential (related to production) and pH should also be included in the model. For reducing the calculation cost, the soil column depth can be reduced as the fast uptake rate, as well as the transport time limits the effects of deeper source and sink.

Moreover, a timestep of 0.5 s in the new Sun model limits the upscaling, while the steady-state solution is fast but not as realistic as the column model. Now that the delaying time of the soil flux's response to the temperature change is around 10 min (Figure 26), it is possible to add some limiting factors to the steady-state solution for

it to reproduce the observed fluxes in the field, thus saves computational time. Another option is to change the discretization method to allow a larger timestep.

Acknowledgements

I would like to first thank my thesis supervisor Prof. Maarten Krol of the Meteorology and Air Quality Group at Wageningen University. He has guided me through the thesis with so much patience, and it was such a pleasure to work with him. He consistently allowed this thesis to be my own work, and encouraged me to try, but steered me in the right direction especially when I got lost in the details.

I would also like to thank the my peers in the MAQ thesis ring 1 for giving me feedback on writing, as well as for those inspiring discussion. Also I would like to thank others who have provided me with their help during this academic year.

I would like to thank my friends in MAQ whom I spent the thesis time with: Antje, Bernice, Emily, Gayan, Maarten, Mark, Xuemei... for all the support and chocolate that they have given to me through these few months.

Finally, I must express my very profound gratitude to my parents and to my best friend Kate for providing me with unfailing support and continuous encouragement throughout my years of study. This accomplishment would not have been possible without them.

Thank you.

Enpei Li

References

[1] R. K. Pachauri, M. R. Allen, V. R. Barros, J. Broome, W. Cramer, R. Christ, J. A. Church, L. Clarke, Q. Dahe, P. Dasgupta, Climate change 2014: synthesis report. Contribution of Working Groups I, II and III to the fifth assessment report of the Intergovernmental Panel on Climate Change, IPCC, 2014.

[2] J. Campbell, G. Carmichael, T. Chai, M. Mena-Carrasco, Y. Tang, D. Blake, N. Blake, S. Vay, G. Collatz, I. Baker, Photosynthetic control of atmospheric carbonyl sulfide during the growing season, Science 322 (5904) (2008) 1085–1088.

[3] G. Flato, J. Marotzke, B. Abiodun, P. Braconnot, S. C. Chou, W. J. Collins, P. Cox, F. Driouech, S. Emori, V. Eyring, Evaluation of climate models. in: Climate change 2013: The physical science basis. contribution of working group i to the fifth assessment report of the intergovernmental panel on climate change, Climate Change 2013 5 (2013) 741–866.

[4] J. Grace, M. Rayment, Respiration in the balance, Nature 404 (6780) (2000) 819.

[5] T. Launois, P. Peylin, S. Belviso, B. Poulter, A new model of the global biogeochemical cycle of carbonyl sulfide-part 2: Use of carbonyl sulfide to constrain gross primary productivity in current vegetation models, Atmospheric Chemistry and Physics 15 (16) (2015) 9285.

[6] S. F. Watts, The mass budgets of carbonyl sulfide, dimethyl sulfide, carbon disulfide and hydrogen sulfide, Atmospheric Environment 34 (5) (2000) 761–779.

[7] A. Engel, U. Schmidt, Vertical profile measurements of carbonylsulfide in the stratosphere, Geophysical research letters 21 (20) (1994) 2219–2222.

[8] M. Chin, D. Davis, Global sources and sinks of ocs and cs2 and their distributions, Global Biogeochemical Cycles 7 (2) (1993) 321–337.

[9] A. Kettle, U. Kuhn, M. Von Hobe, J. Kesselmeier, M. Andreae, Global budget of atmospheric carbonyl sulfide: Temporal and spatial variations of the dominant sources and sinks, Journal of Geophysical Research: Atmospheres 107 (D22).

[10] M. Berkelhammer, D. Asaf, C. Still, S. Montzka, D. Noone, M. Gupta, R. Provencal, H. Chen, D. Yakir, Constraining surface carbon fluxes using in situ measurements of carbonyl sulfide and carbon dioxide, Global Biogeochemical Cycles 28 (2) (2014) 161–179.

[11] M. E. Whelan, T. W. Hilton, J. A. Berry, M. Berkelhammer, A. R. Desai, J. E. Campbell, Carbonyl sulfide exchange in soils for better estimates of ecosystem carbon uptake, Atmospheric Chemistry and Physics 16 (6) (2016) 3711–3726.

[12] G. Protoschill-Krebs, C. Wilhelm, J. Kesselmeier, Consumption of carbonyl sulphide (cos) by higher plant carbonic anhydrase (ca), Atmospheric Environment 30 (18) (1996) 3151–3156.

[13] L. Sandoval-Soto, M. Kesselmeier, V. Schmitt, A. Wild, J. Kesselmeier, Observations of the uptake of carbonyl sulfide (cos) by trees under elevated atmospheric carbon dioxide concentrations, Biogeosciences 9 (8) (2012) 2935.

[14] S. Schenk, J. Kesselmeier, E. Anders, How does the exchange of one oxygen atom with sulfur affect the catalytic cycle of carbonic anhydrase?, Chemistry-A European Journal 10 (12) (2004) 3091–3105.

[15] J. Berry, A. Wolf, J. E. Campbell, I. Baker, N. Blake, D. Blake, A. S. Denning, S. R. Kawa, S. A. Montzka, U. Seibt, A coupled model of the global cycles of carbonyl sulfide and co2: A possible new window on the carbon cycle, Journal of Geophysical Research: Biogeosciences 118 (2) (2013) 842–852.

[16] U. Seibt, L. Wingate, J. Lloyd, J. Berry, Diurnally variable δ18o signatures of soil co2 fluxes indicate carbonic anhydrase activity in a forest soil, Journal of Geophysical Research: Biogeosciences 111 (G4).

[17] K. Maseyk, J. A. Berry, D. Billesbach, J. E. Campbell, M. S. Torn, M. Zahniser, U. Seibt, Sources and sinks of carbonyl sulfide in an agricultural field in the southern great plains, Proceedings of the National Academy of Sciences 111 (25) (2014) 9064–9069.

[18] J. Ogée, J. Sauze, J. Kesselmeier, B. Genty, H. Van Diest, T. Launois, L. Wingate, A new mechanistic framework to predict ocs fluxes from soils, Biogeosciences 13 (8) (2016) 2221–2240.

[19] W. Sun, K. Maseyk, C. Lett, U. Seibt, A soil diffusion–reaction model for surface cos flux: Cossm v1, Geoscientific Model Development 8 (10) (2015) 3055–3070.

[20] T. Deepagoda, P. Moldrup, P. Schjønning, L. W. d. Jonge, K. Kawamoto, T. Komatsu, Density-corrected models for gas diffusivity and air permeability in unsaturated soil, Vadose Zone Journal 10 (1) (2011) 226–238.

[21] H. Van Diest, J. Kesselmeier, Soil atmosphere exchange of carbonyl sulfide (cos) regulated by diffusivity depending on water-filled pore space, Biogeosciences 5 (2) (2008) 475–483.

[22] F. E. Moyano, S. Manzoni, C. Chenu, Responses of soil heterotrophic respiration to moisture availability: An exploration of processes and models, Soil Biology and Biochemistry 59 (2013) 72–85.

[23] P. Moldrup, T. Olesen, T. Komatsu, S. Yoshikawa, P. Schjønning, D. Rolston, Modeling diffusion and reaction in soils: X. a unifying model for solute and gas diffusivity in unsaturated soil, Soil Science 168 (5) (2003) 321–337.

[24] R. Horn, A. Smucker, Structure formation and its consequences for gas and water transport in unsaturated arable and forest soils, Soil and Tillage Research 82 (1) (2005) 5–14.

[25] P. Moldrup, T. Olesen, J. Gamst, P. Schjønning, T. Yamaguchi, D. Rolston, Predicting the gas diffusion coefficient in repacked soil water-induced linear reduction model, Soil Science Society of America Journal 64 (5) (2000) 1588–1594.

[26] R. J. Ferm, The chemistry of carbonyl sulfide, Chemical Reviews 57 (4) (1957) 621–640.

[27] W. Henry, Experiments on the quantity of gases absorbed by water, at different temperatures, and under different pressures, Philosophical Transactions of the Royal Society of London 93 (1803) 29–276.

[28] C. K. Ho, S. W. Webb, Gas transport in porous media, Vol. 20, Springer, 2006.

[29] F. Kitz, K. Gerdel, A. Hammerle, T. Laterza, F. M. Spielmann, G. Wohlfahrt, In situ soil cos exchange of a temperate mountain grassland under simulated drought, Oecologia 183 (3) (2017) 851–860.

[30] M. Von Hobe, R. Najjar, A. Kettle, M. Andreae, Photochemical and physical modeling of carbonyl sulfide in the ocean, Journal of Geophysical Research: Oceans 108 (C7).

[31] J. Kesselmeier, N. Teusch, U. Kuhn, Controlling variables for the uptake of atmospheric carbonyl sulfide by soil, Journal of Geophysical Research: Atmospheres 104 (D9) (1999) 11577–11584.

[32] Y. Liu, H. He, Q. Ma, Temperature dependence of the heterogeneous reaction of carbonyl sulfide on magnesium oxide, The Journal of Physical Chemistry A 112 (13) (2008) 2820–2826.

[33] W. Li, L.-j. Yu, D.-x. Yuan, Y. Wu, X.-d. Zeng, A study of the activity and ecological significance of carbonic anhydrase from soil and its microbes from different karst ecosystems of southwest china, Plant and soil 272 (1-2) (2005) 133–141.

[34] I. M. Unger, A. C. Kennedy, R.-M. Muzika, Flooding effects on soil microbial communities, Applied Soil Ecology 42 (1) (2009) 1–8.

[35] A. Borowik, J. Wyszkowska, Soil moisture as a factor affecting the microbiological and biochemical activity of soil, Plant Soil Environ 62 (6) (2016) 250–255.

[36] J. Sauze, S. P. Jones, L. Wingate, S. Wohl, J. Ogée, The role of soil ph on soil carbonic anhydrase activity, Biogeosciences 15 (2) (2018) 597–612.

[37] M. E. Whelan, R. C. Rhew, Carbonyl sulfide produced by abiotic thermal and photodegradation of soil organic matter from wheat field substrate, Journal of Geophysical Research: Biogeosciences 120 (1) (2015) 54–62.

[38] Y. Mu, C. Geng, M. Wang, H. Wu, X. Zhang, G. Jiang, Photochemical production of carbonyl sulfide in precipitation, Journal of Geophysical Research: Atmospheres 109 (D13).

[39] W. Sun, K. Maseyk, C. Lett, U. Seibt, Litter dominates surface fluxes of carbonyl sulfide in a californian oak woodland, Journal of Geophysical Research: Biogeosciences 121 (2) (2016) 438–450.

[40] W. Van Wijk, Physics of plant environment, Soil Science 98 (1) (1964) 69.

[41] T. Ogawa, K. Noguchi, M. Saito, Y. Nagahata, H. Kato, A. Ohtaki, H. Nakayama, N. Dohmae, Y. Matsushita, M. Odaka, Carbonyl sulfide hydrolase from thiobacillus thioparus strain thi115 is one of the β-carbonic anhydrase family enzymess, Journal of the American Chemical Society 135 (10) (2013) 3818–3825.

[42] J. Berg, J. Tymoczko, L. Stryer, The michaelis-menten model accounts for the kinetic properties of many enzymes, Biochemistry 5.

[43] J. Crank, P. Nicolson, A practical method for numerical evaluation of solutions of partial differential equations of the heat-conduction type, Advances in Computational Mathematics 6 (1) (1996) 207–226.

[44] K. W. Oleson, D. M. Lawrence, B. Gordon, M. G. Flanner, E. Kluzek, J. Peter, S. Levis, S. C. Swenson, E. Thornton, J. Feddema, Technical description of version 4.0 of the community land model (clm).

[45] G. Bonan, B. Drewniak, M. Huang, Technical description of version 4.5 of the community land model (clm), Report, NCAR Technical Note NCAR/TN-503+ STR, Boulder, Colorado (2013).

[46] J. H. Ferziger, M. Peric, Computational methods for fluid dynamics, Springer Science & Business Media, 2012.

[47] A. Kaisermann, J. Ogée, J. Sauze, S. Wohl, S. P. Jones, A. Gutierrez, L. Wingate, Disentangling the rates of carbonyl sulphide (cos) production and consumption and their dependency with soil properties across biomes and land use types, Atmos. Chem. Phys. Discuss. 2018 (2018) 1–27.

[48] J. Liu, C. Geng, Y. Mu, Y. Zhang, Z. Xu, H. Wu, Exchange of carbonyl sulfide (cos) between the atmosphere and various soils in china, Biogeosciences 7 (2) (2010) 753–762.

[49] R. M. Daniel, M. J. Danson, Temperature and the catalytic activity of enzymes: A fresh understanding, FEBS letters 587 (17) (2013) 2738–2743.

[50] R. Eisenthal, M. E. Peterson, R. M. Daniel, M. J. Danson, The thermal behaviour of enzyme activity: implications for biotechnology, Trends in biotechnology 24 (7) (2006) 289–292.

[51] B. H. Jo, I. G. Kim, J. H. Seo, D. G. Kang, H. J. Cha, Engineered escherichia coli with periplasmic carbonic anhydrase as a biocatalyst for co2 sequestration, Applied and environmental microbiology 79 (21) (2013) 6697–6705.

[52] F. Yang, R. Qubaja, F. Tatarinov, E. Rotenberg, D. Yakir, Assessing canopy performance using carbonyl sulfide (cos) measurements, Global change biology.

[53] M. E. Peterson, R. Eisenthal, M. J. Danson, A. Spence, R. M. Daniel, A new intrinsic thermal parameter for enzymes reveals true temperature optima. volume 279 (2004) pages 20717-20722, Journal of Biological Chemistry 280 (50) (2005) 41784–41784.

Appendix A. Appendix

Appendix A.1. Temperature dependency of uptake term in the Sun & the Ogée model

We test the temperature responses of the analytical solution for OCS fluxes for homogeneous soils. To make the parameters comparable, we modified the optimum temperature for enzyme uptake in our model (referred as the Sun model) to the Ogée's formulation, and we refer this new version as "modified Sun". The output of the Ogée model exhibits the same transition from soil sink to source with increasing temperature. The trend of Ogée also shows the soil processes change from uptake dominant to production dominant (Figure A.28(a)).

The temperature dependency in the modified Sun model is described as a function of equilibrium temperature, T_{eq}. T_{eq} is the temperature at which the equilibrium between the active enzyme and an inactive form is reached. However, there is a gap between T_{eq} and optimum temperature for enzyme activity (T_{opt}) (Figure A.28(b)). The T_{opt} is smaller than T_{eq}. We used the equation from classical model of enzyme activity[53] to calculate the T_{eq} we need for the same T_{opt} in the Ogée of 298.15 K, T_{eq} needed is 300.63 K.

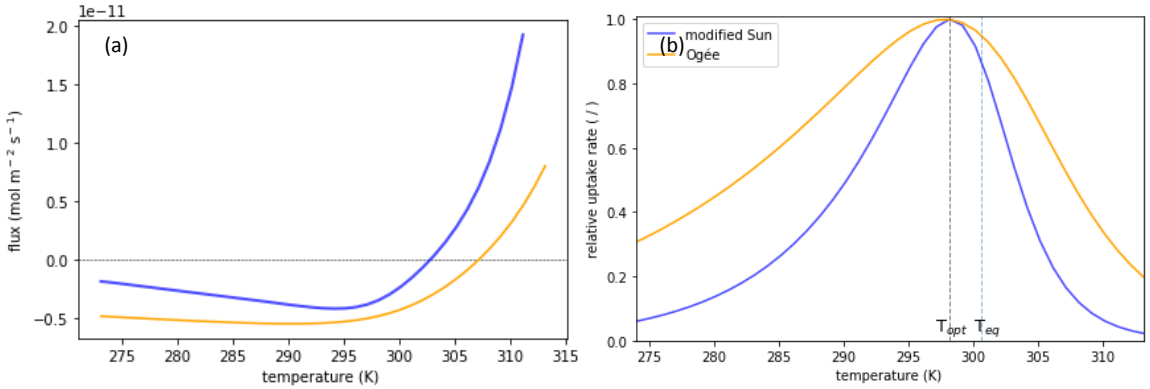

Figure A.28: Comparison between different models' temperature dependency of (a) soil OCS fluxes; (b) relative uptake rate, reflecting the enzyme activity. (fCA=10 000 for the Ogée model).

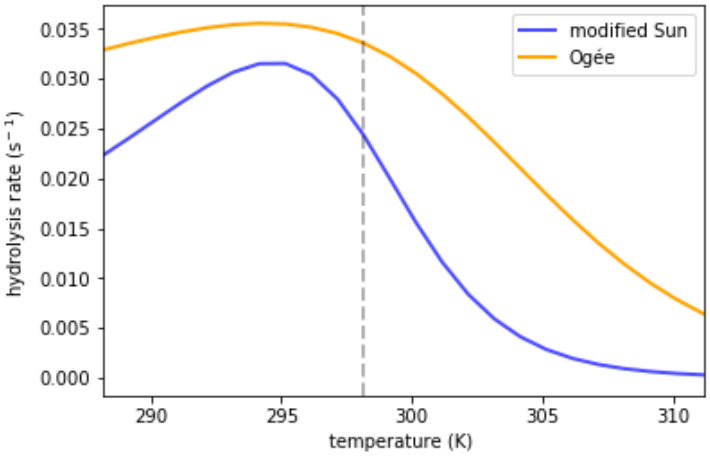

Figure A.29: Comparison between different models' temperature dependency of OCS hydrolysis rate. Dashed line is the optimum temperature for enzyme activity.

Despite the difference of the temperature dependency, we can still reproduce a similar trend of soil OCS fluxes with both models. With increasing T, the soil firstly acts as a sink and is uptake dominant, then after the transition, the soil is production dominant thus acts a source. Then we analyzed the uptake rates of both model to see the cause of difference between the optimum temperatures, noted that the total uptake rate or hydrolysis is the effect of enzymatic uptake and dissolution (Figure A.29).

As the dissolution of OCS is exothermic reaction, we expect a shift of optimum temperature of total uptake rate (k) from that of the enzymatic uptake to left (Figure A.29). Further tuning of the models to make them comparable is in chapter 6.

Appendix A.2. Soil moisture and the sink to source transition

Similar to temperature dependency of the hydrolysis, the moisture dependency is also expected to influence the transition. The optimum soil water content (w_opt) is set to 0.2 for the enzyme in the Sun model. With the effect of dissolution, the max of hydrolysis rate shifts to the left of the w_opt of the Sun model (Figure A.30(a)). Overall for both model, the moisture dependency of hydrolysis rate is similar. Although there is no prescribed w_opt in the Ogée model, by changing the dissolution term, we can manipulate the available OCS for hydrolysis. However, when changing the dissolution term of the Ogée model to the same as the Sun model, there is no significant difference in the simulated OCS soil flux.

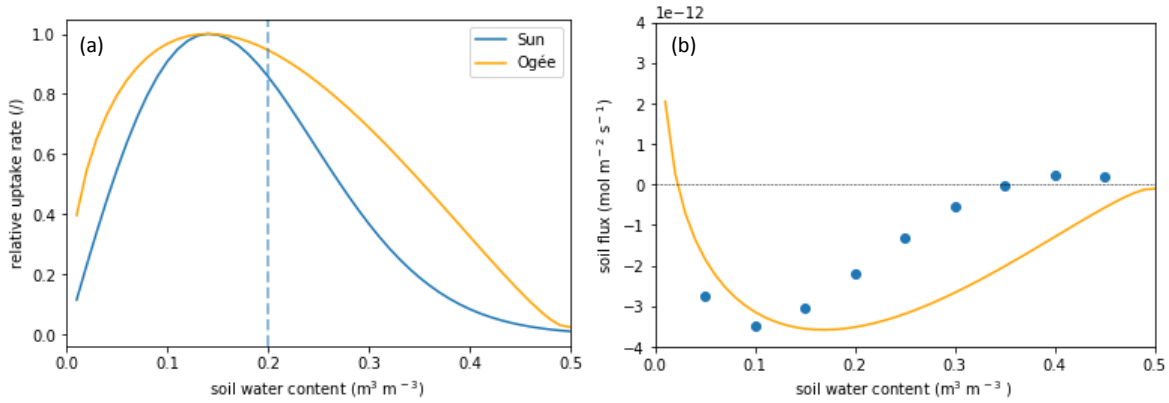

Figure A.30: The relationship between soil water content (porosity=0.5) and (a) OCS relative uptake rate, showing the enzyme activity; (b) soil OCS flux of the Sun model and the Ogée model

Therefore the moisture is important for the OCS soil fluxes. The influence is mainly in its effect to the enzyme activity, and less in dissolution. As the trend of enzyme uptake rate' dependency on moisture in Sun is steeper than that of Ogée, the slope in flux is expected to change more rapidly (Figure A.30(b)). When the whole soil column is filled with water, the diffusivity of the Sun model is by definition zero,); while in the Ogée model, OCS can still diffuse through water in a dissolved form. Therefore when soil water content reaches 0.5, the Sun model shows zero flux, where the Ogée model shows a small negative flux.

The moisture is an important driver for the OCS soil flux mostly by influencing the enzyme activity, and the diffusion can be blocked at high soil moisture.

Appendix A.3. Compensation concentration in the Ogée model

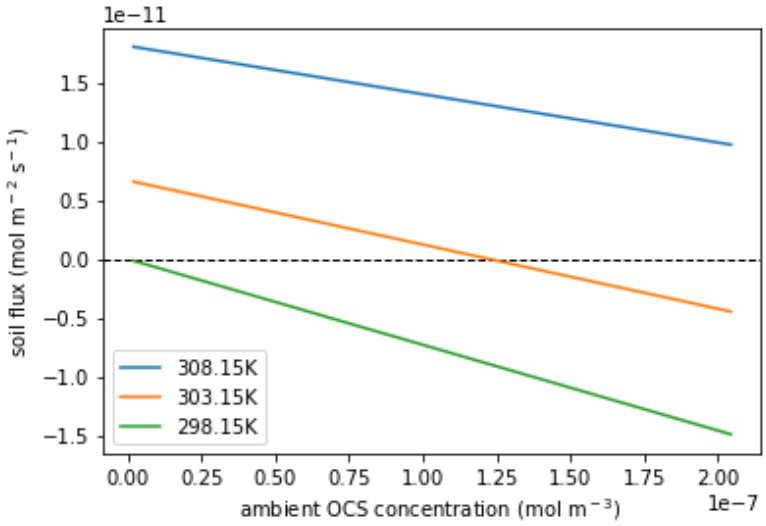

Figure A.31: The relationship between ambient concentration and soil OCS flux in the Ogée model, when temperature is 298.15, 303.15, and 308.15 K in the whole soil column. The black dash line marks the zero flux, at which is the compensation concentration.

Appendix B. Code of the models

```
# -*- coding: utf-8 -*-
#the model including Sun, modifiedSun and newSun model
import numpy as np
class Sun(object):
    def __init__(self):
        self.N = 26
        self.Tref=298.15 #K
        self.R=8.3145
        self.theta_w=0.1 #water-filled porespace
        pressure = 1e5 # Pa
        mV = self.R*298.15/pressure   # m3/mol
        self.Ca = 500e-12/mV#Ca=20.437e-9 #mol/m3#500 ppt#ambient concentration
        n=np.arange(self.N) #arange, tillN-1
        self.z=np.exp(0.2*n-5) #Zi depths of computational nodes
        self.dz=np.zeros(self.N) #delta Zi, thicknessses of control volumes
        self.deltaz=np.zeros(self.N) #delta Zi, Zi-Zi-1
        self.dz[0]=(self.z[0]+self.z[1])*0.5
        self.dz[1:self.N-1]=(self.z[2:self.N]-self.z[0:self.N-2])*0.5
        self.dz[self.N-1]=self.z[self.N-1]-self.z[self.N-2]
        self.deltaz[1:self.N]=self.z[1:self.N]-self.z[0:self.N-1]
        self.deltaz[0]=self.z[0]
        self.zi=np.zeros(self.N+1)#depths of the layer interfaces Z[i+1/2]
        self.zi[1:self.N]=(self.z[0:self.N-1]+self.z[1:self.N])*0.5  #interface
        self.zi[self.N]=1.5*self.z[self.N-1]-0.5*self.z[self.N-2]
        self.psi = -0.5*np.pi
        self.TS=298.15 #set to be Tref #slowly varying component,yearly
        self.TF=10 #10 #fast varying component, set to be 10K for test
        self.zT=0.11 #damping depth for diurnal temperature waves, SGP
        self.omega=np.pi*2/24   #omega=2pi/24 hours
        self.theta=np.zeros(self.N) #theta total porosities, SGP
        mask1=self.z>0.02 #top 2cm 0.60
        self.theta[mask1]=0.50
        mask2=self.z<=0.02
        self.theta[mask2]=0.50#0.60
        self.theta_a=self.theta-self.theta_w
        self.C=np.full(self.N,self.Ca)#=np.zeros(self.N) #filled
        self.Ji=np.zeros(self.N+1)
        self.Di=np.zeros(self.N+1)
        self.Gi=np.zeros(self.N)
        self.gg = np.zeros(self.N+1)
        self.D=np.zeros(self.N)
        self.T=np.zeros(self.N)
        self.kH=np.zeros(self.N)
    def calcDi(self,model):
        '''calculate the diffusivity, dependent on temperature and moisture '''
        if model=='newSun': #'Mol03r'
            D0a = 1.27e-5*np.power(self.T/298.15,1.5) # m2/s from Ogee
            D0lT0=1.94e-9/((298.15/216-1)*(298.15/216-1)) #diffusivity at 261 K
            D0l = D0lT0*(self.T/216-1)*(self.T/216-1) # m2/s
            ta = np.power(self.theta_a,3./2)/self.theta #Mol03r
            tl = np.power(self.theta_w,3./2)/self.theta #Mol03r
            Deffa = D0a*ta*self.theta_a # m2/s air diffusion
            Deffl = D0l*tl*self.theta # diffusion in water
            self.D = Deffa + Deffl*self.kH#Bog
            self.Di[0]=2/(1/self.D[0]+1/D0a[0])#at the interface
            self.Di[1:self.N]=(self.D[1:self.N]+self.D[0:self.N-1])*0.5
        elif model=='Sun'or 'modifiedSun':
            Dmax=1.337e-5
            D0a=Dmax
            b=5.3
```

```
            self.D=Dmax*np.power((self.T/self.Tref),1.5)\
            *np.power((self.theta_a/self.theta),3/b)*np.power(self.theta_a,2)
            self.Di[1:self.N]=(self.D[1:self.N]+self.D[0:self.N-1])*0.5
            self.Di[0]=2/(1/self.D[0]+1/D0a)#at the interface
        else:
            self.Di=np.zeros[:]
        return self.Di
    def calcGi(self):
        '''calculate the conductivity Gi'''
        self.Gi[0]=(self.Di[0]/self.z[0])#derive from equation(7)
        for j in range(1,self.N):
            self.Gi[j]=self.Di[j]/(self.z[j]-self.z[j-1])
        return self.Gi
    def calcT(self,hours,Tmodel):
        ''' calculate temperature profile as a function of simulation hours
        hours = simulted hours, choose from samediurnal, diurnal, constant'''
        if Tmodel=='samediurnal':
            self.T = self.TS + self.TF\
            *np.sin(self.omega*hours + self.psi - 0*self.z/self.zT)
        elif Tmodel=='diurnal':
            self.T = self.TS + self.TF*np.exp(-self.z/self.zT)\
            *np.sin(self.omega*hours + self.psi - self.z/self.zT) #omega*tofday
        elif Tmodel=='constant':
            self.T[:]=self.TS
        else:
            self.T[:]=self.TS
        return self.T
    def calcP(self,model,zero = False):
        '''calculate the production of OCS (Q10)'''
        #if zero == False:
        self.Vsmax = 1e-10
        self.Q10=3
        if model=='newSun':
            self.Q10=3
            P = self.Vsmax*np.power(self.Q10,(self.T-298.15)/10.0)
        elif model=='Sun' or 'modifiedSun':
            self.Q10=1.9
            P = self.Vsmax*np.power(self.Q10,(self.T-298.15)/10.0)
        return P
    def calckH(self,model):
        '''the dimensionless Henry's law constant(dissolution fraction) '''
        if model=='newSun':
            kHog=0.021*np.exp(24900/self.R*(1/self.T-1/298.15)) #mol m-3 Pa-1
            self.kH=kHog*self.R*self.T*0.01
            return self.kH
        elif model=='Sun' or 'modifiedSun':
            alpha=-20.00
            beta=4050.32#from fig2
            self.kH=self.T*np.exp(alpha+beta/self.T)
            return self.kH
        else:
            self.kH=0
    def calcfT(self,model):
        '''calculate the temperature dependency of enzyme activity in Sun
        models, not used in newSun model '''
        deltaG=84.10*1000 #J/mol
        deltaH=358.9*1000 #J/mol, deltaHeq
        fup=self.T*np.exp(-deltaG/(self.R*self.T))
        if model=='modifiedSun':
            self.Teq=300.629
```

```
            fdown=1.+np.exp(-(1./self.T-1/self.Teq)*deltaH/self.R)
            self.fT=20082956711028.02*fup/fdown/8.4873948394548435
        elif model=='Sun':
            self.Teq=273.15+10 #SGP
            fdown=1.+np.exp(-(1./self.T-1/self.Teq)*deltaH/self.R)
            self.fT=20082956711028.02*fup/fdown
        else:self.fT=0
        return self.fT
    def calcg(self,model):
        '''the moisture dependency of the enzyme activity in the Sun model '''
        if model=='newSun':
            self.g=0
        elif model=='Sun' or 'modifiedSun':
            wopt=0.20 #m3/m3 #0.2 for SGP, 0.14 SR
            Aw=0.4665342826418889
            w=self.theta_w
            self.g=Aw*w/(wopt**2)*np.exp(-w**2/(wopt**2))
        else:
            self.g=0
        return self.g
    def calcxCAref(self,model):
        ''' Calculates the referenced xCAref for the
        temperature dependency of enzyme activity '''
        deltaHa=40*1000 #J mol-1
        deltaHd=200*1000 #J mol-1
        deltaSd=660 #J mol-1 K-1
        if model == 'newSun':
            self.xCAref=np.exp(-deltaHa/(self.R*(self.Tref)))\
            /(1+np.exp(-deltaHd/(self.R*(self.Tref))+deltaSd/self.R))
            return self.xCAref
        else:
            self.xCAref=1
            print "xCA not applicable"
    def calcU(self,dt,model):
        Km=1.9
        self.Vumax=1.2e-1
        fCA=3e4
        deltaHa=40*1000 #J mol-1
        deltaHd=200*1000 #J mol-1
        deltaSd=660 #J mol-1 K-1
        pp=-14+4.5#pH 4.5 pkw
        if model=='newSun':
            xCA=np.exp(-deltaHa/(self.R*(self.T)))/\
            (1+np.exp(-deltaHd/(self.R*(self.T))+deltaSd/self.R))
            kuncat=2.15e-5*(np.exp(-10450*(1/self.Tref-1/298.15)))\
            +12.7*np.power(10,pp)*np.exp(-6040*(1/self.Tref-1/298.15))
            k = fCA*kuncat*xCA/self.xCAref
            U=-k*self.kH*self.theta_w*self.C #uptake off
            return U
        elif model=='Sun' or 'modifiedSun':
            U=-self.Vumax*self.kH*self.C/(Km+self.kH*self.C)*self.fT*self.g
            return U
        else:
            U[:]=0.0
            return U
    def calcC(self,U,P,dt):
        ''' Calculates the progression of the concentration in time.
        Takes as arguments,
        dt = timestep in [s]
        U,P, uptake, production rate, in [mol m-3 s-1]'''
```

```
    S=(U+P)*self.dz#the production-loss term
    S[0]=self.Di[0]*self.Ca/self.z[0]+(U[0]+P[0])*self.dz[0]
    eta=self.kH*self.theta_w+self.theta_a
    A=np.diagflat([self.dz*eta],)
    self.gg[0:self.N]=self.Gi
    B=np.diagflat([self.Gi[j] for j in range(1,self.N)], 1)+\
    np.diagflat([self.Gi[j] for j in range(1,self.N)], -1)+\
    np.diagflat([(-self.gg[j]-self.gg[j+1]) for j in range(0,self.N)],0)
    AA=np.linalg.inv(2.*A-dt*B)
    AB=2.*A+dt*B
    BB=AB.dot(self.C)+2.*dt*S
    self.C=AA.dot(BB)
    return  self.C #AA.dot(BB)
def calcJi(self):
    '''flux based on concentration gradient in [mol m-2 s-1], + emission'''
    self.Ji[0]=self.Di[0]*(self.C[0]-self.Ca)/self.deltaz[0]
    self.Ji[1:self.N]=self.Di[1:self.N]\
    *(self.C[1:self.N]-self.C[0:self.N-1])/self.deltaz[1:self.N]
    ##Ji[26] is 0 by definition
    return self.Ji
def runmodel(self,dt,tend,model,Tmodel):
    self.Tarr = []
    self.Tarr0 = []
    self.Parr = []
    self.Garr = []
    self.Carr = []
    self.Carr0 = []
    self.Jarr = []
    self.Farr = []
    self.Uarr = []
    self.Uarr0 = []
    self.kHarr = []
    self.Sarr = []
    self.Darr = []
    self.calcxCAref(model)
    self.g=self.calcg(model)
    self.dtime = []
    xtime = 0.0
    it = 0
    while xtime < tend:
        it += 1
        hours = xtime
        self.T=self.calcT(hours,Tmodel)
        self.kH=self.calckH(model)
        Di=self.calcDi(model)
        self.fT=self.calcfT(model)
        P=self.calcP(model)
        Gi=self.calcGi()
        U=self.calcU(dt,model)
        self.C = self.calcC(U,P,dt)
        xtime +=  dt/3600.0
        if it % 100 == 0:
            dt = min(dt*1.1,20.0)           #time step increasing till 20 s
            #dt=0.5                         #a constant timestep of 0.5 s
            #print(dt)
            self.dtime.append(xtime)
            self.Ji=self.calcJi()
            self.Jarr.append(self.Ji)       #flux
            self.Farr.append(self.Ji[0])    #the surface soil flux
            self.Carr.append(self.C)        #concentration in each layer
```

```
self.Carr0.append(self.C[0])    #concentration at the z[0]
self.Tarr.append(self.T)        #temperature
self.Tarr0.append(self.T[0])    #temperature at the z[0]
self.Parr.append(P)             #production rate [mol m-3 s-1]
self.Uarr.append(U)             #uptake rate in [mol m-3 s-1]
self.Uarr0.append(U[0])         #uptake rate at z[0]
self.Garr.append(Gi)            #conductivity
self.Darr.append(Di)            #diffusivity
```

```
#%%test of the model and the code for the Ogee model
from ocs import *
import numpy as np
import matplotlib.pyplot as plt
d1 = Sun()
d1.runmodel(0.5,72.0,model='newSun',Tmodel='diurnal') #(time step in [s], run time in [h])
e = Sun()
e.runmodel(0.5,72,model='newSun',Tmodel='samediurnal')
#%%Ogee model
f,ax = plt.subplots()
e.Tarr0=np.array(e.Tarr0)
T=e.Tarr0#d1.Tarr0
phi = 0.5
theta = 0.1
ea = phi - theta            # remaining air volume in m3/m3
D0a=1.27e-5*np.power(T/298.15,1.5)  # m2/s from Ogee
D0l25 = 1.94e-9
D0lT0 = D0l25/((298.15/216 - 1.)**2)
D0l=D0lT0*((T/216. - 1.)**2)
ta = np.power(ea,3./2)/phi
tl = np.power(theta,3./2)/phi
Deffa = D0a*ta*ea    # m2/s air diffusion
Deffl = D0l*tl*theta  # diffusion in water
pressure = 1e5 # Pa
pKw = 14.0
kuncat=2.15e-5 * np.exp(-14050.0*(1./298.15 - 1./298.15)) \
+ 12.7*np.power(10,(-pKw+ 4.5))*np.exp(-6040.0*(1./298.15 - 1./298.15) )
R = 8.3145#46 # J/(mol K)
DHa = 40.0e3  # J/mol
DHd = 200.0e3 # J/mol
DSd = 660.0   # J/(mol.K)
xCA=np.exp(-DHa/(R*T))/(1. + np.exp(-DHd/(R*T) + DSd/R))
xCAref=np.exp(-DHa/(R*298.15))/(1. + np.exp(-DHd/(R*298.15) + DSd/R))
Kh=0.021e-2*np.exp(24900*(1./T - 1./298.15)/R)   # now in mol/(m3.Pa)
B=Kh*R*T
D = Deffa + Deffl*B
mV = R*T/pressure   # m3/mol
Ca = 500e-12/mV     # mol COS/m3
fCA =3e4# 30000.0
pH = 8.2#7.2
k = fCA*kuncat*xCA/xCAref
Q10=3
Vsmax=1e-10
P = Vsmax*np.power(Q10,(T -298.15)/10.0)#0.0
z1 = np.sqrt(D/(k*B*theta))
zp = 1#1.09#different depth   # 1m depth
zmax=1
Xi=np.exp(-zmax/z1)
#F = -np.sqrt(k*B*theta*D)*(Ca - (z1*z1*P/D)*(1-Xi*Xi)/(1+Xi*Xi)) #eq.16b
F = -np.sqrt(k*B*theta*D)*(Ca - (z1*z1*P/D)*(1.-np.exp(-zp/z1)))
#%% plotting the comparison of Ogee and newSun model-soil flux
fig,ax2=plt.subplots()
#fig, ax1 = plt.subplots() #plot the temperature change in the first grid point
#ax1.plot(d1.dtime,e.Tarr0, 'r')
#ax1.set_xlabel('time (min)')
#ax1.set_ylabel('temperature (K)', color='r')
#ax1.tick_params('y', colors='r')
#ax1.set_ylim(280,310)
d1.dtime=np.array(d1.dtime)
#ax2 = ax1.twinx()
```

```
d1.Farr=np.array(d1.Farr)
e.Farr=np.array(e.Farr)
ax2.plot(d1.dtime, d1.Farr, 'b',label='diurnal T change with depth')
ax2.plot(d1.dtime, e.Farr, 'b--',label='diurnal T')
ax2.set_ylabel('flux (mol m$^-$$^2$ s$^-$$^1$)', color='b')
ax2.tick_params('y', colors='b')
ax2.set_ylim(-6e-12,6e-12)
ax2.plot(d1.dtime,F,color='orange',label='Ogee')
fig.tight_layout()
plt.legend()
plt.show()
```